NRS
Promoting Science

Review   View Online

Polymers of Intrinsic Microporosity (PIMs) Gas Separation Membranes: A mini Review

Canghai Ma, Jeffrey J. Urban*

The Molecular Foundry, Lawrence Berkeley National Laboratory, 1 Cyclotron Rd, Berkeley, CA 94720, USA
Corresponding Author. Tel.: 510-486-4526; Email: jjurban@lbl.gov

Polymers of Intrinsic Microporosity (PIMs) are broadly recognized as a potential next generation membrane material for gas separations due to their ultra-permeable characteristics. This mini review aims to provide an overview of these materials and capture its very essence, from chemistry to applications. PIMs-based gas separation membranes are divided into three main categories, i.e., neat PIMs, polymer blend PIMs, and mixed matrix PIMs membranes. This review covers a wide spectrum of PIMs with their gas diffusion mechanisms and separation performance, all of which are examined in detail. Core challenges and opportunities of PIMs membrane technology are reviewed, and this article concludes with future perspectives on PIMs. This mini review establishes a comprehensive understanding of the key technological competence and barriers of PIMs for next-generation gas separations membranes.

Significant advances in the science and engineering of membrane materials and separation processes have been witnessed in recent decades. Membranes have demonstrated the capability of reducing the enormous amount of energy consumption for gas separations, compared to conventional thermally driven separation processes, like cryogenic distillation [1]. Indeed, membrane separation process is cost-effective and environmentally friendly with small physical footprints. Interests of membrane technology have been growing increasingly in past decades. Key areas that membranes are at play include CO_2 capture, nitrogen generation, hydrogen/helium recovery, natural gas sequestration and biogas purification [2]. Regarded as a new family of membrane materials, Polymers of Intrinsic microporosity (PIMs) have exhibited extremely high gas separation productivity and drawn extensive attention world-widely. The intrinsic microporosity leverages PIMs membranes to far exceed the Robeson upper bound limit of polymeric membranes, which opens an entirely new avenue for gas separations [3]. This review addresses the key developments and advances of PIMs as a super-permeable membrane material for gas separations. Specifically, this paper presents a comprehensive overview of three imperative types of PIMs membranes: those made from, respectively, neat PIMs, polymer blend PIMs, and mixed matrix PIMs.

1.1 PIMs overview

PIMs are defined as polymers that possess "a continuous network of interconnected intermolecular voids" with pores of less than 2 nm in diameter, formed "as a direct consequence of the shape and rigidity of the component macromolecules" [4]. In the initial design, the aromatic rings in PIMs are fused together so that the polymer chains cannot rotate along the backbone direction and the packing of polymers to a more "condensed" state (i.e. less free space between polymer chains) is strictly restrained. The loss of rotational freedom

and inefficient packing of polymer chains enables PIMs to assume a rigid and contorted molecular configuration. As a result, a large number of pores and high fractional free volume is imparted into the PIMs matrix, leading to Brunauer-Emmett-Teller (BET) surface areas as high as 800 m²g⁻¹. Due to this high surface area and porosity, PIMs can be tailored for multiple applications, such as gas separation, gas storage and catalysis [4].

The idea of PIMs was traced back to Prof. McKeown's work on phthalocyanine materials conducted at Cardiff University in the 1990s [4]. Historically, his group designed a spirocyclic phthalocyanine insoluble network polymer via reaction of a spirocyclic bisphthalonitrile to obtain catalytic activity for oxidation reactions. Serendipitously, PIMs were discovered during a control experiment in the phthalocyanine work. To determine phthalocyanine formation efficiency, the group designed a solution-processable non-network polymer through the dibenzodioxin polymerization of spirocyclic 5,5,6,6-tetra-hydroxy-3,3,3,3–tetramethylspirobisindane and 2,3,5,6-tetra-fluoroterephthalonitrile. This material had a BET surface area of 800 m²g⁻¹ and was later named as PIM-1 in 2004 with the repeat unit shown in **Figure 1** [4]. In principle, PIM-1 was synthesized through a nucleophilic aromatic substitution reaction between hydroxylated aromatic monomers and fluorinated aromatic monomers.
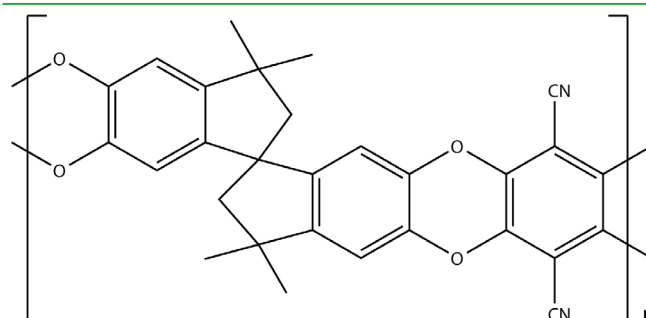

Figure 1. Repeat unit of PIM-1 [4].

Shortly after the discovery of PIM-1, Prof. Budd at the University of Manchester utilized PIM-1 to produce pervaporation membranes for phenol/water separations [5]. PIM-1 is considered as the most well-known PIMs as it is based on commercially available monomers with simple structures, high molecular weight and decent mechanical properties.

During the past two decades, PIMs have been investigated as a new class of extremely permeable membrane materials. PIMs have demonstrated amenable solution-processability and gas permeability far beyond conventional polymers, as will be closely examined in Sections 2.1-2.3. Tremendous resources have been devoted to developing new PIMs-based membranes. Key areas of advance of PIMs as gas separation membranes includes: i) modification and functionalization of PIMs polymer chains to manipulate gas separation properties; ii) blending PIMs with other inexpensive industrially available polymers to finely tailor membrane performance and manufacturability; and iii) mixing PIMs with fillers to prepare hybrid mixed matrix membranes with unique and synergistic properties. These PIMs, including their structures and gas separation behaviors, will be explored thoroughly in this paper to provide a completed overlook and understanding of such a crucial material.

1.2 Applications of PIMs

As a microporous solution-processable membrane material, PIMs have demonstrated astonishing gas separation performance by surpassing the productivity-selectivity tradeoff curve, the so-called upper bound popularized by Robeson [3]. The Robeson upper bound refers an empirical relationship between gas permeability and selectivity of membrane materials, where a more permeable membrane tends to have a lower gas selectivity, and vice versa [6]. PIMs were also employed as pervaporation membranes (the first application of PIMs membranes as mentioned above) and organic solvent nanofiltration membranes. Besides broad application in membranes, PIMs were made into sensors, for instance, PIM-3 was used as an optical sensor for ethanol [7]. Other applications of PIMs include chemoselective adsorbents, heterogeneous catalysts and hydrogen storage [8-10].

1.3 Gas transport mechanisms in membranes

As mentioned earlier, conventional polymers suffer from the Robeson upper bound, a tradeoff between productivity and selectivity. It is important to understand the basic principles involved in the molecular transport in membranes to design PIMs bypassing the upper bound limit of traditional polymer membranes. Based on the material and fabrication process, membranes are generally divided into three categories: (i) neat polymer membranes; (ii) polymer blend membranes; and (iii) mixed matrix membranes. Equations governing gas molecule transport through each type of membranes are explained below.

1.3.1 Gas permeation in polymeric membranes

For gas separations in pure polymeric membranes, the classical solution-diffusion model is most widely accepted as a means to describe gas transport in the membranes [11]. In this model, gas molecules sorb in the membrane upstream and then diffuse through the membrane due to chemical potential differences across the membrane induced by the partial pres-

sure or fugacity differences. The gas mixture finally desorbs in the downstream of membranes. Separation of a gas mixture is realized through the membrane as a result of different solubilities and diffusivities of gas molecules in the membrane, the thermodynamic and kinetic factor, respectively. The gas separation productivity of a dense film membrane is defined by the permeability, P, which is the production of diffusivity, D, and solubility, S, via Eq. (1):

$$P = D \cdot S \qquad (1)$$

The permeability of penetrant i, P_i, is determined by the gas permeation flux of penetrant i, n_i, normalized by the membrane thickness, l, and the partial pressure or fugacity difference, Δp_i, across the membrane, viz.,

$$P_i = \frac{n_i \cdot l}{\Delta p_i} \qquad (2)$$

The common unit of permeability adapted in membrane community is called Barrer, where,

$$1 \ \text{Barrer} = 10^{-10} \left(\frac{\text{cc(STP)} \cdot \text{cm}}{\text{cm}^2 \cdot \text{s} \cdot \text{cmHg}} \right) \qquad (3)$$

For asymmetric hollow fiber membranes with the structure will be shown in 9, a completely different conuration from dense film membranes, the separation productivity is determined by the permeance, P_i/l, which is the pressure or fugacity difference normalized flux of permeant, i, through Eq. (4).

$$\frac{P_i}{l} = \frac{n_i}{\Delta p_i} \qquad (4)$$

The unit of permeance is the GPU, defined in Eq. (5):

$$1 \ \text{GPU} = 10^{-6} \left(\frac{\text{cc(STP)}}{\text{cm}^2 \cdot \text{s} \cdot \text{cmHg}} \right) \qquad (5)$$

In Eq. (4), P_i is the permeability of a dense film membrane made from the same material as hollow fiber membranes; l is the effective selective skin layer thickness of hollow fibers; Δp_i is the transmembrane partial pressure (or fugacity) differences across the hollow fiber wall. The pressure differences must be replaced with the fugacity differences to accurately quantify the true separation performance of the membrane under high pressure operation conditions.

On the other hand, the membrane selectivity, α_{ij}, describes the separation efficiency of a membrane, determined by the ratio of permeability or permeance of the fast gas, i, to the slow gas, j, via Eq. (6):

$$\alpha_{ij} = \frac{P_i}{P_j} = \frac{P_i/l}{P_j/l} \qquad (6)$$

1.3.2 Gas permeation in polymer blend membranes

Polymer blend membranes are formed by mixing two distinctive polymers into one membrane matrix. Blending polymers simultaneously utilizes advantages of each individual polymer in order to create unique and synergistic gas separation properties. It is a cost- and time-effective approach to finely tune the membrane performance as the blended polymer is usually commercially available and inexpensive. Depending on their nature, the two polymers in polymer blends are miscible, immiscible or partially miscible. A miscible polymer blend is homogenous with only one phase, where the two polymers are completely interpenetrated with each other. On
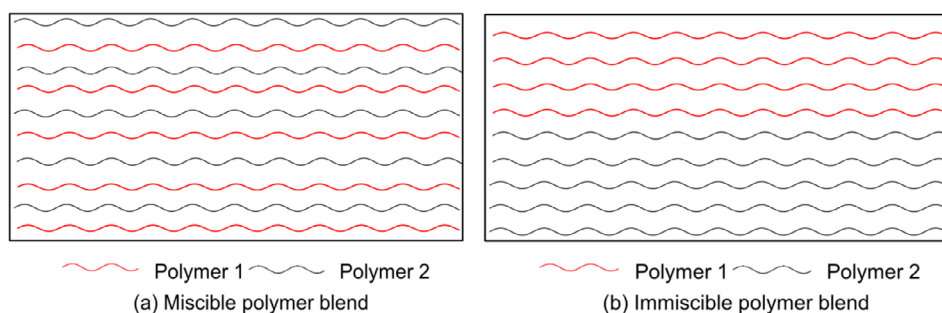
Figure 2. Schematic showing microstructural differences between (a) miscible and (b) immiscible polymer blend. Wiggly lines represent two polymers (red line for polymer 1 and grey line for polymer 2). The two polymers of a miscible polymer blend (a) are completely interpenetrated with each other. An immiscible blend (b) has minor interpenetration of polymer chains in the interphase.

the other hand, an immiscible blend has two phases and only minor interpenetration of polymer chains exists in the interphase. **Figure 2** depicts the key differences between miscible and immiscible polymer blend.

Depending on the miscibility of two polymers, gas permeation behavior of polymer blend membranes is simulated by different models. In the case of two miscible polymers, the permeability of blend membranes follows an empirical relationship with the individual component via the following equation [12]:

$$ln\,P_b = \varphi_1 lnP_1 + \varphi_2 lnP_2 \qquad (7)$$

where P_b, P_1, and P_2 refer the permeability of the blend membrane and constitutive polymer 1 and 2 in its neat format, respectively. $\varphi1$ and $\varphi2$ denote the respective volume fraction of polymer 1 and 2, respectively. The separation efficacy of a polymer blend membrane is determined by the ratio of permeability for a gas pair, as described in Eq. (6).

In the case of partially miscible or immiscible (or phase separated) polymers, prediction of gas transport is somewhat complicated. Several models, including the parallel model, series model, and Maxwell model, were proposed to describe the gas permeation in polymer blend membranes [13]. Among those models, the model in Eq. (7) provided a better estimation than Maxwell model in some cases [14, 15], which therefore was chosen in this section. This fact notwithstanding, Maxwell model was frequently used in simulating gas transport in mixed matrix membranes, as will be discussed in Section 1.3.3.

The miscibility of two polymers is often checked through optical measurements or Differential Scanning Calorimetry (DSC) experiments. Phase separation can be easily found by polarized light microscope as the boundary layer of the interface is apparent under microscope [16]. On the other hand, a homogeneous phase with two miscible polymers demonstrates a single glass transition temperature (Tg) while an immiscible heterogeneous system consisting two immiscible polymers displays two distinctive Tg [12]. The study of Tg evolution serves an effective technique to explore the miscibility of two polymers.

1.3.3 Gas permeation in mixed matrix membranes

To further advance membrane performance, another effective and straightforward approach is via preparing mixed matrix membranes, which consists of two phases, a continuous polymer phase and dispersed particulate phase. Several groups

have reported mixed matrix membranes crossing the upper bound for many different types of separations, as revealed in **Figure 8** (will be discussed in Section 2.3).

Gas transport mechanism through mixed matrix membranes is a complicated subject due to the hybrid and heterogeneous nature of such composite membrane. To simulate ideal gas diffusion in mixed matrix membranes, several models, such as the Maxwell, Bruggeman, Lewis–Nielse and Cussler models, have been proposed and applied for systems with different loadings and morphologies of fillers [17]. Among them, Maxwell model is popularly used as an effective and quantitative method to fit gas permeation in a mixed matrix.

The Maxwell principle dates back to 1873 when Maxwell defined the dielectric constant, or called permittivity, of a dielectric as the factor of proportion between the electric displacement and the electric field or potential gradient [18]. In the case of mixed matrix membranes, the gas permeation flux is proportional to the pressure difference or potential gradient and the permeability is the factor of the proportion. It is assumed that the pressure is continuous across any interface between two phases, i.e., the continuous phase and dispersed phase. Analogous to the permittivity of heterogeneous dielectrics, one can predict permeability of a mixed matrix membrane by replacing the permittivity with permeability in the continuous and dispersed phases in the equation. For a low loading of spherical fillers, the permeability, P_c, of a mixed matrix membrane is described by Maxwell approximation below [18]:

$$P_c = P_m \frac{P_f \cdot (1+2\varphi_f)+P_m \cdot (2-2\varphi_f)}{P_f \cdot (1-\varphi_f)+P_m \cdot (2+\varphi_f)} \qquad (8)$$

P_m and P_f are the permeability of the continuous phase and dispersed filler phase, respectively, in the mixed matrix membrane. refers the volume fraction of filler in the membrane. It was assumed that the loading of dispersants is sufficiently low so that the gas diffusion pattern around a particle is not affected by its surrounding particles and the particle-particle interaction is negligible. A particle loading up to 30% was fitted into Maxwell model and found to approximate gas permeabilities [19]. However, it is important to note that the assumption of negligible particle-particle interaction and inhomogeneity of mixed matrix are the main reasons that cause deviated or failed prediction of gas permeabilities using Maxwell model.

Similar to the neat polymer and polymer blend membranes, the gas separation selectivity of a mixed matrix membrane is defined by the ratio of permeability of a given gas pair, as described in Eq. (6).
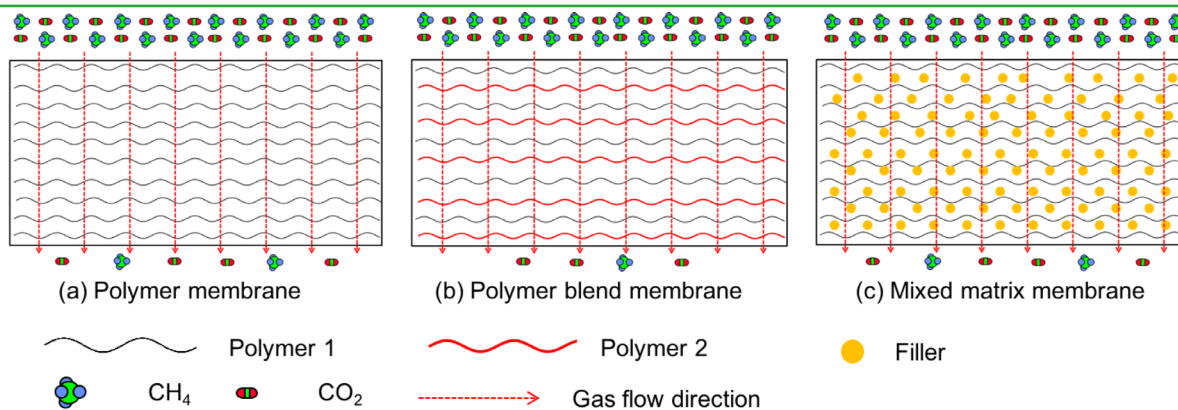
Figure 3. Schematic describing three gas diffusion processes through (a) polymer membrane, (b) polymer blend membrane, and (c) mixed matrix membrane. Feed gas example: CO_2/CH_4 pair. Wiggly lines represent polymer chains (the grey color refers polymer 1 and the red refers polymer 2). Red dashed lines depict gas flow direction.

To summarize gas transport mechanisms in membranes, the gas transport processes through the three kinds of PIMs-based membranes can schematically depicted in **Figure 3**, using CO_2/CH_4 gas pair as a feeding gas mixture. In **Figure 3**, the red and grey wiggly lines represent two polymers and the orange dots indicate the filling materials in mixed matrix membranes. Red dashed lines depict gas flow directions. As shown in **Figure 3** (a), polymer membranes follow the solution-diffusion model and the feeding CO_2/CH_4 molecules are dissolved and diffuse in the membrane and get separated in the permeate side. In the case of PIMs-based polymer blend membranes, as **Figure 3**-(b) depicts, the incorporation of another less permeable but more selective polymer into PIMs membrane (red line) usually benefits gas selectivity with some reduction of flux, as will be examined in Section 2.2. For the mixed matrix membrane in **Figure 3**-(c), the fillers (orange dots) establish a percolation network, leading to a synergistic enhancement of both permeability and selectivity in some cases. Such unique feature of mixed matrix membranes will be reviewed in Section 2.3.

2 PIMS MEMBRANES FOR GAS SEPARATIONS

2.1 Neat PIMs membranes

Gas separation membranes can be prepared from neat PIMs, meaning only one PIM polymer is used in the membrane without mixing any other additives, like nanoparticles. In the recent two decades, extensive PIMs membranes were developed by altering constitutive monomers of PIMs, such as functionalization of polymer chains or introducing new monomers. The resulting polymers demonstrated intrinsic microporosity through creating either spirobiindane (SBI)-based or non-SBI-based sites with bulky pendant groups. SBI refers a unique molecule, consisting of two indanes connected by a spiro carbon center. Here, an indane contains a benzene ring attached by a five-membered or six-membered ring. A typical SBI unit is shown in **Figure 4**. Some monomers were made from Tröger's Bases and polyimides. PIMs membranes based a single polymer are generally categorized into five types as will be reviewed in the following Sections 2.1.1-2.1.5.

2.1.1 Basic SBI-based PIMs

The first kind of neat PIMs membranes is formed with a SBI-centered A-B type PIMs, where A and B represent aromatic tetrol monomer and halogen-containing aromatic monomer repeating units (such as fluorinated or chlorinated), respectively. A-B PIMs is synthesized through dibenzodioxane formation of two monomers (e.g. A and B monomer) wherein small gas molecules, such as hydrogen fluoride, are released as by-products during reaction. PIM-1 represents the first example of SBI-centered PIMs with monomer 5,5,6,6-tetra-hydroxy-3,3,3,3-tetramethylspirobisindane (monomer A) and 2,3,5,6-tetrafluoroterephthalonitrile (monomer B) shown in **Figure 5** [4].

Since the discovery of PIM-1, new hydroxylated aromatic monomers with SBI-centers were synthesized to prepare novel PIMs. PIMs-based on 1,1-spiro-bis(1,2,3,4-tetrahydronaphthalene) monomer were developed in 2009 [20]. The five-membered spiro aromatic rings on polymer A were replaced by six-membered rings and the pending groups attached the benzene rings were also modified. A large family of SBI-based PIMs was reported afterwards to significantly expand the spectrum of PIMs [4]. Chemical structures of typical tetrolhydroxlyated (A monomer) and bi-halogen-containing (such as fluorinated or chlorinated, B monomer) aromatic monomers
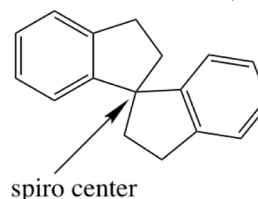

Figure 4. Chemical structure of typical SBI units with benzene rings attached by five-carbon rings connected by a spiro carbon center, where the rings do not possess rotation freedom and form a rigid structure.
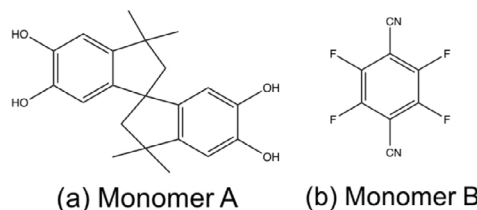

(a) Monomer A   (b) Monomer B

Figure 5. Chemical structures of (a) Monomer A: 5, 5, 6, 6-tetrahydroxy-3, 3, 3, 3-tetramethylspirobisindane and (b) Monomer B: 2, 3, 5, 6-tetrafluoroterephthalonitrile of PIM-1 [4].
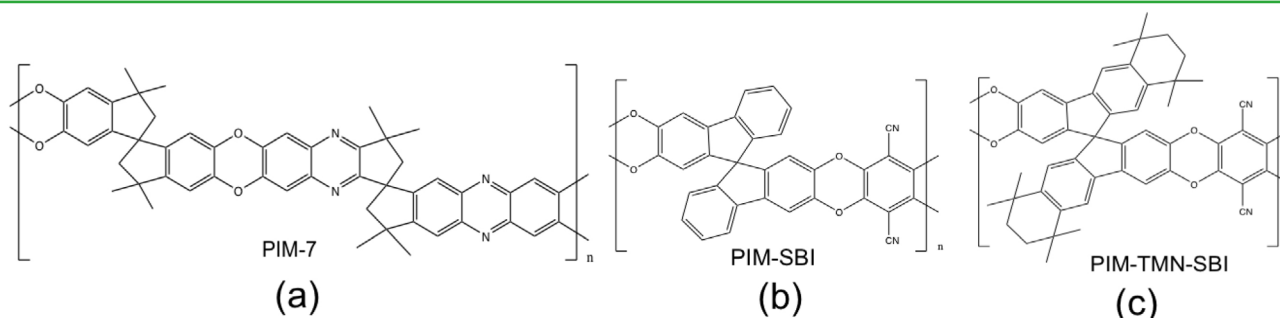
Figure 6. Structures of SBI-centered PIMs: (a) PIM-7, (b) PIM-SBI and (c) PIM-TMN-SBF for gas separations with gas separation performance shown in **Table 2** [21, 22]. Note that those PIMs contain SBI units and rings are fused together, prohibiting the rotation of polymer chains.

to prepare neat SBI-based PIMs are summarized in **Table 1**. Here, B monomers can contain both halogen and SBI centers in some cases.

Despite dozens of monomers reported to synthesize SBI-based PIMs, only a few of such PIMs were made into gas separation membranes, including PIM-1, PIM-7, PIM-Spiro-bifluorene (SBF) and PIM-TMN-SBF [21-23] (TMN-SBF: 2,2',3,3'-Tetrahydroxy-6,6,6',6',9,9,9',9'-octamethyl-6,6',7,7',8,8',9,9'-octahydro-11,11'-spiro-bi[cyclohexa[b]fluorine). This clearly suggests there is plenty of headspace for further preparing neat PIMs membranes. Their chemical structures are depicted in **Figure 1, 5** (PIM-1) and **Figure 6**.

2.1.2 Tröger's Base-based PIMs

Tröger's Base (TB) was firstly synthesized and reported in 1887 and studied for fields such as supramolecular chemistry and catalysis [24]. TB unit was recently incorporated into PIMs network via TB polymerization and produced a so-called TB-PIMs membrane. Most of the TB-based monomers are single bi-amino aromatic polymers with SBI or without SBI-centers. Bi-amino aromatic polymers with bicyclic rings, such as ethanoanthracene (EA) and triptycene (Trip), can form a rigid and contorted network with SBI centers in the presence of dimethoxymethane in trifluoroacetic acid [25]. TB-PIMs were also synthesized through reacting TB-embedded tetrol-hydroxy aromatic monomers and 2,3,5,6-tetrafluoroterephthalonitrile [26]. After its first application in membranes, several bi-amino aromatic monomers were used to obtain TB-based PIMs with structures listed in **Figure 7** and **Table 1** [27-29].

The gas separation properties of typical TB-based PIMs membranes are described in **Table 2**. Note that PIM-EA-TB, PIM-Trip-TB and PIM- Benzotriptycene (BTrip)-TB represent three examples of super permeable PIMs membranes in this category, exhibiting separation performance well above the upper bound [24, 30]. Clearly, TB-based PIMs have become an important branch of PIMs membranes, deserving our attention.

2.1.3 Polyimide-based PIMs

PIMs-based on polyimide (PI) were heavily studied in recent years. Polyimides, formed via polycondensation of anhydrides and diamines, are a new generation of permeable membrane materials offering high gas separation performance, easy processability and manufacturability. Following the similar synthesis route as polyimide, anhydrides and diamines with functional groups can react through polycondensation to produce a series of PI-based PIMs. Due to the relatively flexible nature and high Tg of polyimides, integrating polyimide groups into PIMs increases polymer robustness, improves solvent solubility and leads to separation performance surpassing the upper bound [30]. It is also worthy to mention that the unique functionalities and polymer properties render PI-PIMs a rich class of derivatives via thermal treatments, such as thermally rearranged (TR) and carbon molecular sieves (CMS) [15, 31].

PI-PIMs are generally divided into three categories: 1) PIMs made from reaction of dianhydride with contortion sites, such as SBI, EA and Trip, and halogen-containing aromatic diamines without contortion sites [32-36]; ii) PIMs prepared through dianhydride without contortion sites but diamines with contortions sites, such as SBI, TB, Trip, and pentiptycene[37-44]; iii) PIMs formed via TB polymerization of single di-amino aromatic monomer with imide bonds and contortion sites [45-47]. PI-PIMs with contorted sites in both dianhydride and TB-based diamine units were seldom reported [48]. PI-PIMs were thermally treated to obtain TR-PIMs, such as
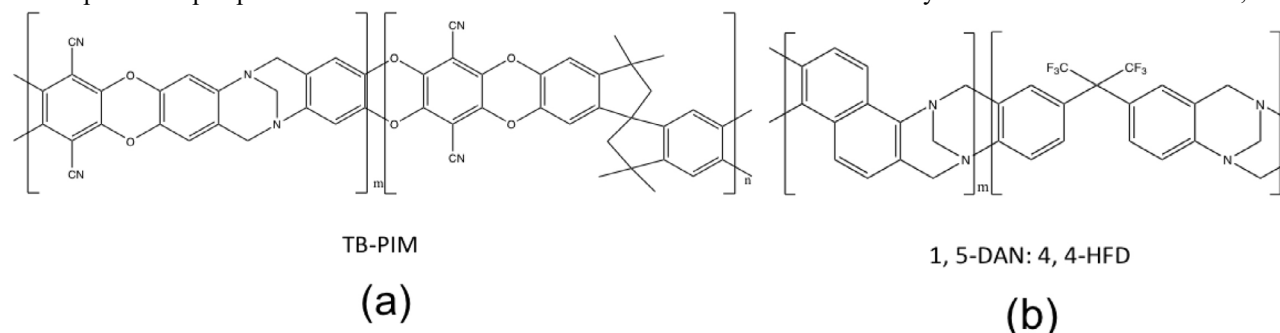

Figure 7. Chemical structures of two TB-based PIMs membranes (a) TB-PIM and (b) 1, 5-diaminonaphathelen (DAN)/4, 4-(Hexafluoroisopropylidene) dianiline (HFD) PIM [26, 29]. Some of other TB-based PIMs, including PIM-EA-TB, PIM-SBI-TB, PIM-Trip-TB, and PIM-2,2-bis (3-methyl-4-aminophenyl) adamantine (Ad-Me) are shown in **Table 1**.

Table 1. Chemical structures of PIMs monomers/PIMs. Notes: 6FDA: 4, 4′-(hexafluoroisopropylidene) diphthalic anhydride; BTDA: 3,3′,4,4′-benzophenonetetracarboxylic dianhydride.

PIMS	Chemical structures of monomers/PIMs
Basic SBI-based PIMs	
TB -based PIMs	

Table 1 (*Continued*)
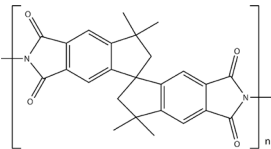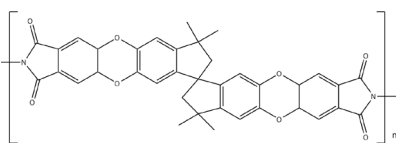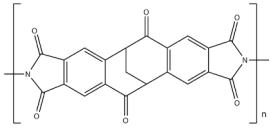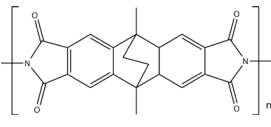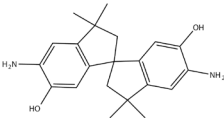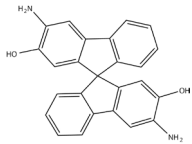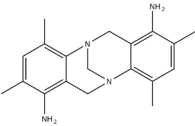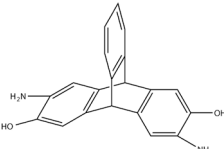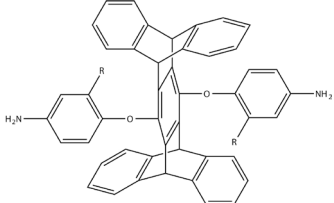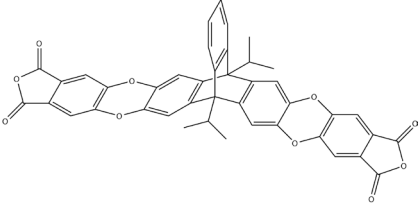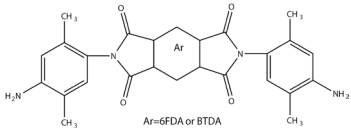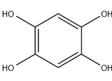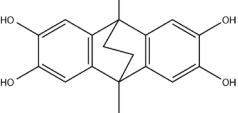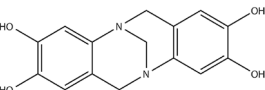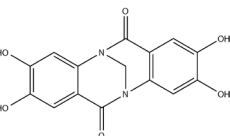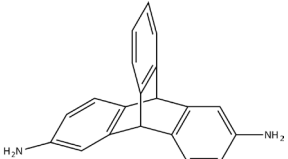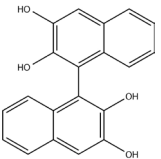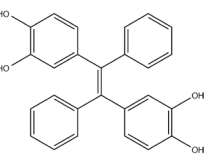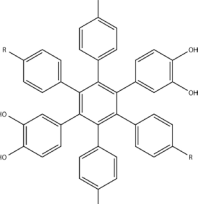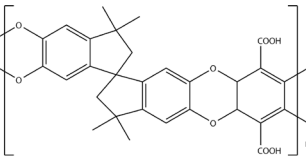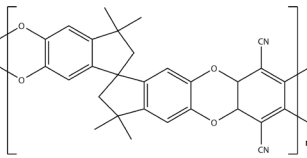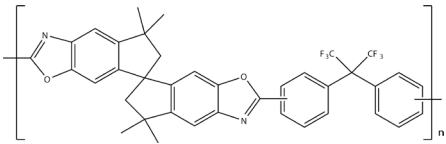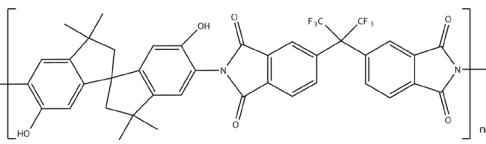
PIMS	Chemical structures of monomers/PIMs		
Polyimide-based PIMs			
Non-SBI-based PIMs			
PIMs with thermal treatment			

Table 2. Gas permeation properties of neat PIMs membranes. Permeation data were adapted based on pure gas permeation unless specified. *Alcohol treated. TPDA-mPDA: 9,10-diisopropyl-triptycene-based dianhydride (TPDA), TPDA-m-phenylenediamine (mPDA); CTB1-DMN: 5,6,11,12-tetrahydro-5,11-methanodibenzo[a,e] [8] annulene-2,3,8,9-tetracarboxylic anhydride (CTB1), 3,3′-dimethylnaphthidine (DMN); SPDA-HSBF: Spirobisindane-based dianhydride (SPDA), 2,2′-dihydroxyl-9,9′-spiro-bifluorene-3,3′-diamine (HSBF); TBDA2-6FDA-PI: 3,9-diamino-4,10-dimethyl-6H,12H-5,11-methanodibenzo[1,5]- diazocine (TBDA2); 4MTBDA−SBIDA: 2,8-diamino-1,3,7,9-tetramethyl-6H,12H-5,11-methanodibenzo[b, f][1,5] diazocine (4MTBDA), spirobisindane-based dianhydride (SBIDA); 6FDA-DAT1-OH: 2,6 (7)-dihydroxy-3,7(6)-diaminotriptycene (DAT1-OH); DC-PIM1: decarboxylated-PIM1; TOX-PIM-1: thermal-oxidatively crosslinked PIM-1; PIM-(Na-1d): sodium hydrolyzed PIM for 1day.

PIMs type	PIMs Name	Testing conditions	Permeability (P_i, Barrer)				Selectivity ($\alpha_{i/j}=P_i/P_j$)					Reference
			H_2	He	O_2	CO_2	α_{H_2/N_2}	α_{He/N_2}	α_{O_2/N_2}	α_{CO_2/N_2}	α_{CO_2/CH_4}	
Basic SBI-based PIMs	PIM-1	30 °C, 0.2 bar	1300	660	370	2300	14.1	7.2	4.0	25	18.4	[23]
	PIM-1	30 °C, 1 bar*	3300	1320	1530	11200	5.4	2.2	2.5	18.4	9.7	[99]
	PIM-1	35 °C, 4 bars	2332	1061	786	3496	9.8	4.5	3.3	14.7	9.7	[114]
	PIM-1	25 °C, 3.4 bars, 40 min*	3042	1114	1133	5366	8.6	3.1	3.2	15.2	NA	[115]
	PIM-1	25 °C, 3.4 bars, 120 min *	3364	1531	1560	7329	6.7	2.8	2.9	13.4	NA	[115]
	PIM-1	25 °C, 3.4 bars*	3847	-	1717	7108	6.1	-	2.7	11.3	NA	[116]
	PIM-1	25 °C, 1 bar*	5010	1950	2270	13600	6.1	2.4	2.8	16.6	10.0	[117]
	PIM-1	25 °C, 1 bar	2936	1340	969	5303	11.7	5.3	3.8	21.0	16.6	[105]
	PIM-7	30 °C, 0.2 bar	860	440	190	1100	20	10.5	4.5	26.0	17.7	[23]
	PIM-SBF	25 °C, 1 bar*	6320	2200	2640	13900	8.1	2.8	3.4	17.7	12.6	[21]
	PIM-TMN-SBI	25 °C, 1 bar*	7190	2720	3200	17500	6.7	2.5	3.0	16.2	8.3	[22]
TB-based PIMs	PIM-EA-TB	25 °C 1 bar*	7760	2570	2150	7140	14.8	4.9	4.1	13.6	10.2	[24]
	PIM-SBI-TB	25 °C 1 bar*	2200	878	720	2900	9.4	3.8	3.1	12.5	6.4	[24]
	PIM-Trip-TB	25 °C 1 bar*	8039	2500	2718	9709	12.8	4.0	4.3	15.9	10.7	[30]
	TB-PIM25	35 °C 1 bar	-	-	917	4441	-	-	3.5	17.0	11.8	[26]
	TB-Ad-Me	25 °C, 1 bar*	1800	-	437	1820	14.9	-	3.6	15.1	11.2	[28]
Polyimide-based PIMs	PIM-PI-8	30 °C, 0.2-0.5 bar	1600	660	545	3700	10	4.1	3.4	23	14.2	[118]
	PIM-PI-SBI	25 °C, 1 bar	2650	1000	1195	8210	6.0	2.3	2.7	18.7	9.8	[119]
	KAUST-PI-1	35 °C, 2 bars	3983	1771	627	2389	37.2	16.6	5.9	22.3	22.8	[33]
	PIM-PI-EA	25 °C 1 bar*	4230	1580	1380	7340	11.5	4.3	3.7	19.9	16.1	[35]
	TPDA-mPDA	35 °C, 2 bars	431	251	65	349	33.2	19.3	5.0	26.8	31.7	[34]
	CTB1-DMN	35 °C, 2 bars	1295	-	320	1661	17.0	-	4.2	21.8	17.4	[36]
	PIM-6FDA-OH	35 °C, 1 or 2 bars	259	-	45.2	263	24.0	-	4.2	24.0	29.0	[39]
	SPDA-HSBF	35 °C, 2 bars	519	-	98	568	21.6	-	4.1	23.7	19.6	[37]
	TBDA2-6FDA-PI	35 °C	390	223	47	285	32.5	18.6	4.0	23.8	35.6	[40]
	4MTBDA−SBIDA	NA*	3200	-	1132	5140	8.6	-	3.0	13.8	8.7	[43]
	6FDA-DAT1-OH	35 °C, 2 bars	127	-	14	70	47.0	-	5.2	25.9	50.0	[41]
	PI-TB-1	35 °C, 1 bar	607	376	119	457	19.0	12.1	3.8	14.7	16.9	[45]
Non-SBI-based PIMs	HPB-PIM-2	NA	723	340	217	1730	10.9	5.1	3.3	26.1	14.2	[120]
	HPB-PIM	25 °C, 1 bar*	1413	592	534	3800	7.4	3.1	2.8	20.0	10.5	[54]
	PIM-TMN-Trip	25 °C, 1 bar*	16900	6370	7470	33300	7.6	2.9	3.3	14.9	9.7	[22]
PIMs with thermal treatment	PIM-300−2.0d	35 °C, 3.5 bars	3872	-	582	4000	40.3	-	6.1	41.7	54.8	[55]
	DC-PIM1	25 °C, 3.4 bars	-	-	554	2345	-	-	3.4	14.6	12.2	[59]
	TOX-PIM-1	22 °C, 4 bars, 385 °C 1hr crosslinked	2979	-	1013	5100	10.6	-	3.6	18.1	16.9	[57]
	PIM-(Na-1d)	35 °C, 2 bars	-	-	1339	5112	-	-	2.8	10.6	10.4	[56]
	PIM-UV 20min	35 °C, 3.5 bars	2818	-	416	1869	38.3	-	5.7	25.4	30.1	[64]
	spiroTR-PBO-6F	35 °C, 1 bar	429	318	120	675	14.3	10.6	3.9	22	20	[49]
	PIM-1-UV-10min	22 °C, 4 bars	2986	-	1097	6374	10.1	-	10.1	21.6	16.2	[65]
	SPDA-SBF-PBO	35 °C, 2 bars	775	-	225	1280	12.5	-	3.7	20.8	15.1	[37]
	PIM-PBO-1	25 °C, 1 bar*	881	479	226	1176	13.8	7.5	3.5	18.0	17.0	[66]
	PIM-6FDA-OH- CMS	35 °C, 2 bars	5248	-	1071	5040	28.4	-	5.8	27.2	38.0	[63]

PIM-TR-polybenzoxazoles (PBO) [49]. In summary, PI-PIMs take advantages of both flexibility of polyimides and rigidity of PIMs, representing a critical family of PIMs to fabricate high performing neat PIMs membranes and their derivatives.

2.1.4 Non-SBI-based PIMs

The non-SBI-based PIMs refer any PIMs without SBI sites in hydroxyl aromatic monomer moieties, which may overlap with some of TB or PI-based PIMs in Section 2.1.2-2.1.3. Thus, this section will focus on non-SBI-based PIMs without involving with TB and PI monomers. A key feature of non-SBI-based PIMs is that the rigid backbone with contortion sites can be achieved through introducing: i) planar aromatic rings, ii) bicyclic rings or iii) bulky pendant groups, as shown in **Table 1** [4, 50]. Note that the bicyclic rings are mostly EA or Trip and involved with forming contorted TB units, such as PIM-EA-TB and PIM-Trip-TB [35, 51], already discussed in Section 2.1.2. However, hydroxyl aromatic monomers with bicyclic rings can react with fluorinated aromatic monomers, such as 2, 3, 5, 6-tetrafluoroterephthalonitrile, to prepare PIMs without formation of TB units [22, 52]. Bulky side groups containing aromatic rings were used in PIMs to hinder polymer chain rotation and create contorted sites [50, 53]. For example, hexaphenylbenzene (HPB) was added to PIMs (PIM-HPB) to render a disrupted structure and therefore enhance gas permeability significantly [54]. Synthesis of SBI-based PIMs and non-SBI-based PIMs can involve multiple steps with complicated chemistry and controllable functionalities. However, non-SBI based PIMs using of EA or Trip bicyclic rings generally create rather frustrated microstructures, which can yield membranes with higher gas permeability than the case of SBI-based PIMs with short side chains. The two approaches whether using SBI unit or not are both viable and represent different techniques in making desirable PIMs.

2.1.5 PIMs with thermal or UV treatment

Several PIMs have been cross-linked to create a more robust framework via thermal treatment attempting to augment CO_2 plasticization resistance without prohibitively sacrificing high permeable characteristic of PIMs. Two main approaches were hypothesized to prepare cross-linked PIMs, self-cross-linking and cross-linker assisted cross-linking. Self-cross-linking was accomplished by thermal cross-linking and Ultraviolet (UV)-assisted cross-linking, while cross-linker assisted cross-linking includes chemical cross-linking and metal ion cross-linking [55-59]. PIM-1 was postulated to be self-cross-linked under 300 $^{\circ}$C to form triazine rings among nitrile group with metal ions [55]. The nitrile groups facilitated formation of a cross-linked network through decarboxylation cross-linking with or without hydrolysis of nitrile groups under moderate temperatures [57, 59]. Some researches presumed PIMs were cross-linked by adding cross-linkers, such as diazides[60, 61], beta-cyclodextrin (CD) [62] and intermolecular polycyclic aromatic hydrocarbons (PAHs) [58]. Under even higher temperature (above 530 $^{\circ}$C), PIM-1 and hydroxyl PIMs (PIM-6FDA-OH) were pyrolyzed to fabricate CMS membranes [63].

UV exposure was utilized to enhance gas selectivities of PIMs with some corresponding loss of permeability. Several mechanisms were assumed to rationalize the function of UV via thermally rearrangement or photo-oxidation of surface [37,

49, 64-67]. The wide range of PIMs derivatives via thermal or UV treatment indeed diversifies the family of PIMs membranes by offering performance unobtainable in their untreated formats. PIMs precursors to form PIMs derivatives via thermal or UV treatment were summarized in **Table 1**.

To conclude neat PIMs, the aforementioned five categories of PIMs are not completely distinguished from each other, rather, some of which correlate, or even overlap, to some degree. As **Table 1** demonstrates, the spectrum of PIM monomers is enormously vast and new PIMs are created by matching monomers with different functionalities. Neat PIMs membranes are straightforward to be prepared without complication caused by dopants, such as blending polymer or nanoparticles which will be illustrated in Section 2.2-2.3. Gas separation performance of neat PIMs membranes are summarized in **Table 2**. Certain PIMs membranes have demonstrated separation performance beyond the upper bound such as PIM-EA-TB, PIM-TMN-SBF and PIM-Trip-TB [22, 24, 30]. The processability of using PIMs was also improved by introducing flexible polyimide groups. The thermal or UV treatment on PIMs enhanced the plasticization resistance in the presence of condensable species, like CO_2. Overall, neat PIMs constitute the vital part of PIMs with the most diverse monomers and functionalities [68]. Future innovation on monomer structures and functionalization of PIMs is definitely desirable and technically important.

To further push the envelope of separation upper bound and manufacturability of PIMs membranes, techniques through blending polymers or nanoparticles were excessively investigated, which will be examined in detail in following Sections 2.2 and 2.3.

2.2 Polymer Blend PIMs membranes

Blending one polymer with another polymer provides an effective alternative to boost the overall gas separation performance of polymer membranes. Since PIMs are intrinsically ultra-permeable with permeability significantly higher than conventional polymers, blending PIMs with other less permeable polymer will inevitably cause loss of flux with some increase of selectivity. When blending a less permeable polymer 2 into PIMs (polymer 1), based on model in Eq. (7), assuming $P_2 << P_1$ and a small fraction of polymer 2 in the blend (e.g. $\varphi_2 << 1$), the term $\varphi_2 ln P_2 << \varphi_1 ln P_1$, which is negligible and Eq. (7) is simplified into the following:

$$lnP_b \cong \varphi_1 lnP_1$$

Since $\varphi_1 < 1$, so $P_b \cong P_1 \wedge \varphi_1 < P_1$, which means the permeability (P_b) of PIMs polymer blend is lower than the neat PIMs membranes, In rare scenarios, some extremely porous polymers were blended into PIMs membrane matrix, leading to an increase of permeability, such as hyper-crosslinked polymers (HCPs) [69].

The polymer blending technique was most employed in recent years with only a handful of literature reported in the field. PIMs were doped with conventional polymers to fabricate polymer blend PIMs membranes to increase membrane mechanical properties and manufacturability. The polymers for blending were mostly polyimides, for instance, Matrimid® [15], Torlon® [11, 70], P84 [71] and Ultem [14]. Other blending polymers include poly (ethylene glycol) (PEG) [72], Polyhedral Oligomeric Phenethyl-silsesquioxanes [73], HCPs

[69], polyphenylenesuflone (PPSU) [16] and etc. As will be discussed in Section 3.3, PIMs is only soluble in particular solvents and have limited miscibility with conventional polymers, which hinders the selection of blending materials. Despite the limited spectrum of blending materials, blending allows further tailoring of PIMs membrane gas permeability and selectivity by simply mixing another complementary polymer. Blending materials and gas separation of blend PIMs membranes is described in **Table 3**.

As **Table 3** signifies, although several commercially available inexpensive polymers are blended into PIMs membranes with promising gas separation performance, a predominant challenge is that those polymers have limited miscibility with PIMs. To reach full potentials of blending technique, the loading of polymers is expected to be sufficiently high to offset high cost of PIMs, which may essentially result in a lower performance or even a failed membrane. For instance, 10% Matrimid® in PIMs caused an incremental increase of fluxes but its immiscibility with PIMs is apparent, indicative of a potential manufacturing issue [15]. While blending polymers can control membrane properties, from a pragmatic point of view, the ultimate goal of blending is to reduce the cost of mem-

brane fabrication without prohibitive loss of flux. Increasing the loading of blending polymer without considerably losing the high separation performance of PIMs remains a technical challenge. Future work should focus on the development of new compatible inexpensive polymers with improved miscibility and loading, thereby reducing the PIMs membrane manufacturing cost while maintaining attractive separation performance.

2.3 PIMs-based mixed matrix membranes (MMMs)

Another effective technique to further push the boundary of PIMs membrane gas separation is through fabricating mixed matrix membranes. A great variety of materials, including both inorganic and organic/inorganic hybrid, were embedded into PIMs polymer matrix to facilitate gas transport due to controlled pore sizes permitting fast diffusion and molecular sieving of similarly sized gas molecules [74]. The versatile pore sizes and functionalities of doping materials allow fine tuning of gas permeabilities and selectivities. The local polymer dynamics in the mixed matrix, such as stiffness, segmental chain motion and fractional free volume, is adjustable by the embed-

Table 3. Gas permeation properties of polymer blend PIMs membranes, compared with Matrimid® and polysulfone. Maximum and minimum loading of polymers are selected if different loadings were studied. All data are adapted based on pure gas permeation unless specified. Notes: C-PIM-1: Carboxylated-PIM-1; PPSU: Polyphenylenesulfone.

| PIMs	Blending polymer	Loading (wt%)	Testing conditions	Permeability (P_i, Barrer)			Selectivity ($\alpha_{i/j}=P_i/P_j$)				Reference
				H$_2$	O$_2$	CO$_2$	α_{H_2/N_2}	α_{O_2/N_2}	α_{CO_2/N_2}	α_{CO_2/CH_4}	
PIM-1	Matrimid®	5	35 °C, 3.5 bars	-	632	3355	-	3.8	20	14	[15]
PIM-1	Matrimid®	95	35 °C, 3.5 bars	-	2.6	12	-	6.6	29	35	[15]
C-PIM-1	Matrimid®	5	35 °C, 3.5 bars	1568	445	2268	13.0	3.7	18.7	13.3	[121]
C-PIM-1	Matrimid®	95	35 °C, 3.5 bars	41.8	3.1	13.6	87.1	6.4	28.3	34.9	[121]
PIM-1	Ultem	5	35 °C, 3.5 bars	-	557	3276	-	3.6	21.1	11.8	[14]
PIM-1	Ultem	95	35 °C, 3.5 bars	-	0.6	2.2	-	7.0	26.2	36.5	[14]
C-PIM-1	Torlon®	5	35 °C, 3.5 bars	1044	244	1382	15.5	3.6	20.5	16.0	[70]
C-PIM-1	Torlon®	95	35 °C, 3.5 bars	4.3	0.2	0.7	188.0	7.1	29.7	40.1	[70]
PIM-1	P84	10	35 °C, 3.5 bars	-	-	2061	-	-	-	20.4	[71]
PIM-1	P84	70	35 °C, 3.5 bars	-	-	7.0	-	-	-	31.7	[71]
PIM-1	PEG	0.5	30 °C, 4-12 bars	-	-	3125	-	-	16.1	17.8	[72]
PIM-1	PEG	5	30 °C, 4-12 bars	-	-	2551	-	-	12.9	26.0	[72]
PIM-1	POSS-PEG	1	30 °C, 1 bar	-	-	3360	-	-	18	13	[73]
PIM-1	POSS-PEG	10	30 °C, 1 bar	-	-	1309	-	-	31	30	[73]
PIM-1	PPSU	5	35 °C, 3.5 bars	2783	1047	5763	7.7	2.9	16.0	10.5	[16]
PIM-1	PPSU	15	35 °C, 3.5 bars	1670	599	2550	9.1	3.3	13.9	12.3	[16]
PIM-1	HCP	4.76	25 °C, 2 bars	-	-	10125	-	-	12.2	-	[69]
PIM-1	HCP	16.67	25 °C, 2 bars	-	-	19086	-	-	11.6	-	[69]
Matrimid®	-	-	35 °C, 3.5 bars	-	2.1	10	-	6.6	31.3	35.3	[95]
Polysulfone	-	-	35 °C, 10 bars	14.0	1.4	5.6	55.9	5.6	22.4	22	[94]
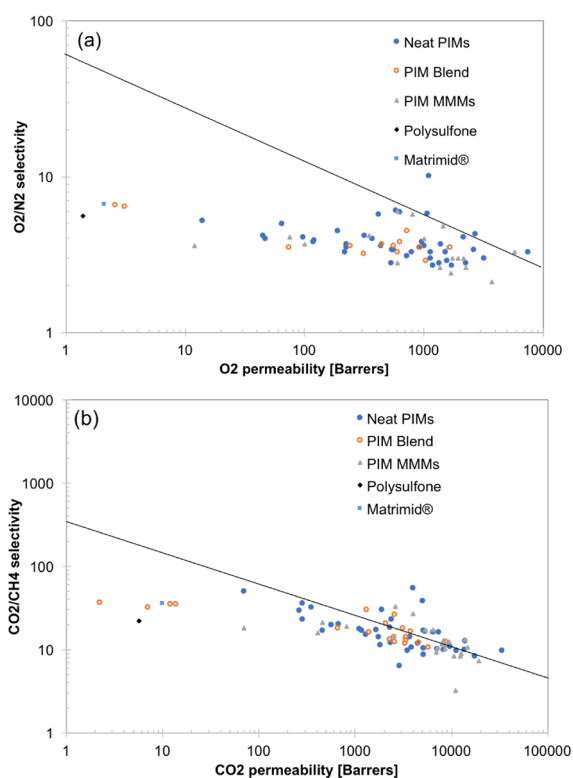
Figure 8. (a) O_2/N_2 and (b) CO_2/CH_4 separation performance of PIMs membranes with current upper bound of polymers. Conventional polymeric membranes, polysulfone and Matrimid® membranes, are plotted for comparison [94, 95].

ded filler. The synthetic design principle enables PIMs MMMs unprecedented performance far beyond the upper bound.

The fillers used in PIMs-based MMMs are divided into three main categories: i) inorganics, such as silica, carbon nanotube, graphene, metal salt etc.; ii) metal-organic complex, such as Zeolitic Imidazolate Frameworks (ZIF)-8, ZIF-71, UiO-66, Copper 1,4-benzenedicarboxylate (CuBDC); iii) organic solids, such as Covalent Organic Framework (COF). Note that the third type of MMMs excludes polymer blend PIMs membranes discussed in Section 2.2, where polymer components in polymer blends are often dissolvable in common solvents. On contrary, the organic solid in mixed matrix membrane, like COF, is a cross-linked network insoluble in regular solvents.

Inorganic fillers for mixed matrix membranes are generally non-porous, creating free volume in the mixed matrix membranes to increase gas permeability. Silica was firstly reported as an inorganic filling PIMs mixed matrix membranes due to its small size and ready availability [75, 76]. It was also employed in cross-linked PIMs [77]. Since the usage of silica, carbon nanotubes and carbon nitride were doped into PIMs membranes [78-80]. As a new generation of inorganics, graphene was also incorporated in PIMs MMMs [81]. Metal ions were added in PIMs as a cross-linking agent to modulate gas separation performance by creating a cross-linked network to enhance plasticization resistance [82]. Ionic liquids have also been mixed into PIMs membranes [83].

Metal-organic frameworks (MOFs) haves emerged as an important hybrid nanocrystal with broad applications in areas like gas separation, gas storage, catalysis, gas sensor and so on. MOFs are porous crystals, and have precisely controlled pore sizes, enabling facilitated gas diffusion and specific siev-

ing of similarly sized gas molecules. ZIF-8 is a relatively new class of MOFs with extraordinary gas separation properties and strong chemical and thermal stability. The pore size of ZIF-8 is 3.4 Å, making it an excellent molecular sieve for separating gas pairs like CO_2/CH_4 and CO_2/N_2. The kinetic diameters of CO_2, N_2 and CH_4 are 3.3 Å, 3.6 Å, and 3.8 Å respectively, near the aperture size of ZIF-8. ZIF-8 was used in preparing all kinds of MMMs, including PIMs MMMs [77, 84]. In addition, UiO-66 is another family of MOFs with a relatively large aperture (6.0 Å) and stable in harsh chemical and thermal conditions. It was recognized as an outstanding dispersant in fabricating PIMs mixed matrix membranes to greatly enhance gas permeability without significant loss of selectivities [85-88]. Other MOFs were also mixed into PIMs MMMs, such as MIL101, ZIF-71, HKUST-1 and CuBDC [89-92].

The last kind of doping agent to prepare PIMs MMMs is the organic solid. The organic solid is referring a polymer with a network structure insoluble in common solvents, like THF. Blending organic solids into membranes mainly increase the porosity, thereby improving gas permeability. As a typical organic solid, COF is a porous 2D or 3D crystalline with diverse application in fields including gas storage, energy harvesting, CO_2 capture and so on. COF was recently doped into PIMs to fabricate MMMs with enhanced permeability [93].

Overall, the MMM technology enables a wide range selection of filling materials into PIMs membranes and further tuning membrane properties. Fillers in PIMs MMMs and their gas separation are depicted in **Table 4**. As **Table 4** depicts, mixed matrix membranes represent an advanced hybrid membrane configuration with unique and synergistic gas separation properties, some of which have surpassed the upper bound appreciably, as will be discussed in **Figure 8**. Despite the enhancement of separation performance, key challenges associated with MMMs technology include interfacial adhesion and particulate dispersion, which have been immensely reviewed in literatures [17].

To summarize the three PIMs membranes, numerous and unique monomers and tunable functionalities have been extensively investigated in order to prepare novel PIMs membranes. They have been broadly used to prepare a large spectrum of membranes, including both neat and hybrid membranes, many of which have overcome the upper bound limit. Gas separation of PIMs-based membranes are plotted in **Figure 8**, compared with some conventional polymeric membranes, such polysulfone [94] and Matrimid® [95].

2.4 PIMs hollow fiber membranes

Primarily, researchers have concentrated on flat-sheet dense film format of PIMs membranes for academic research. However, hollow fiber membranes are the industrially preferred membrane format for gas separations due to their high surface-volume ratio, as compared to flat-sheet membranes. Hollow fiber membranes possess a thin skin layer with an open porous supporting layer underneath the skin in a tubular morphology, as shown in **Figure 9**. A gas mixture is fed either through the bore side or shell side of the hollow fiber, and the gases permeate through the membrane wall and are separated in the permeate side. Such a unique feature of membrane configuration has positioned hollow fibers the industrial standard membrane products (or so-called hollow fiber membrane
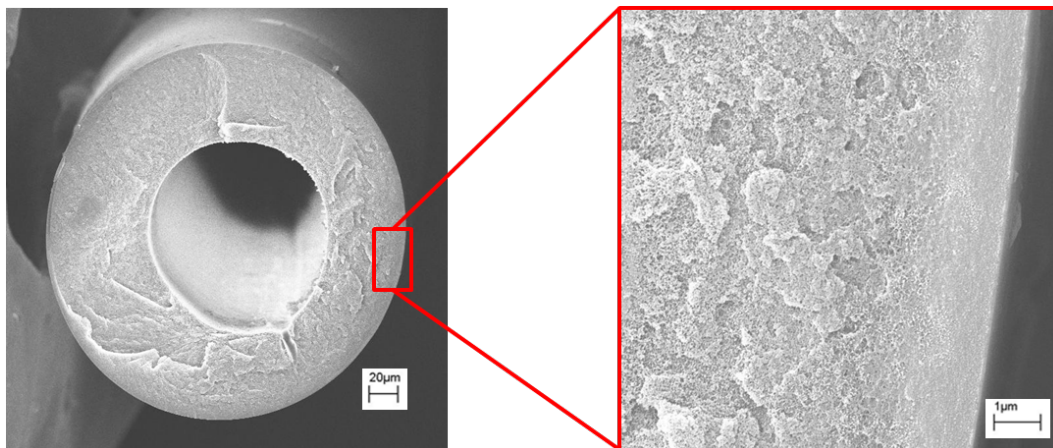
Figure 9. Schematic showing the structure of a hollow fiber membrane consisting of a selective skin layer in the outermost layer of the fiber and an open porous substructure underneath the skin [113].

bundles). Hollow fibers are often manufactured through a phase-invasion dry-jet wet-quench spinning processes [11].

To date, literature reports of PIMs hollow fiber membranes are very limited. Matrimid® and Ultem were blended with PIM-1 to prepare polymer blend hollow fibers membranes [96, 97]. Neat PIM-1 hollow fiber membranes were also fabricated [98]. Gas separation properties of PIM-1 related membranes and membranes from other polymers are compared in **Table 5**. Undoubtedly, more research is deserved to achieve PIMs hollow fiber membranes and their scale-up if they are intended for pragmatic application of gas separations in a large scale.

3 CHALLENGES OF PIMS MEMBRANES AND MITIGATION THEREOF

PIMs-based membranes have exhibited huge potential for gas separations, some of which have surpassed the Robeson upper bound, as depicted in **Figure 8**. Despite their inherently high gas separation potentials, there are challenges associated with developing workable PIMs for separations. Besides the technical difficulties briefed in Section 2, future work should be devoted in following key areas to advance PIMs technology to a higher level. These key challenges are discussed below.

3.1 Physical aging

Physical aging is a prominent issue in porous polymer membranes; aging is a catch-all term that describes the gradual loss of permeability and performance of these systems over time. Aging is believed to be caused by the non-equilibrium nature of the glassy polymer with unrelaxed fractional free volume, which tends to shrink to a more equilibrium (condensed) state over time. Physical aging is an apparent challenge for PIMs membranes due to their high fractional free volume, which undermines the applicability of PIMs for membrane separation. Rapid loss of fluxes leads to unstable performance, which poses another practical operational variable for process control as a steady state of separation is interrupted by the service time. Commercial membranes also experience physical aging, however, the degree of aging of which is significantly lower than that of PIMs.

Many researchers have investigated the physical aging of PIMs [99-101]. Budd et al found a significant loss of gas permeability of PIM-1 in about a week with some increase of gas permselectivity [99]. Tiwari et al also observed rapid loss of O_2 permeability of PIM-1 with data shown in **Figure 10**. Much work has focused on attempts to suppress rapid physical aging of PIMs membranes with some successes achieved in retarding the aging. Approaches to mitigate PIMs aging include UV treatment [67], thermal cross-linking [55] and doping with porous materials, such as porous aromatic framework (PAF) [102], HCP [69], Polyhedral Oligomeric Silsesquioxane (POSS) [103]. Beta-cyclodextrin (CD) was also embedded
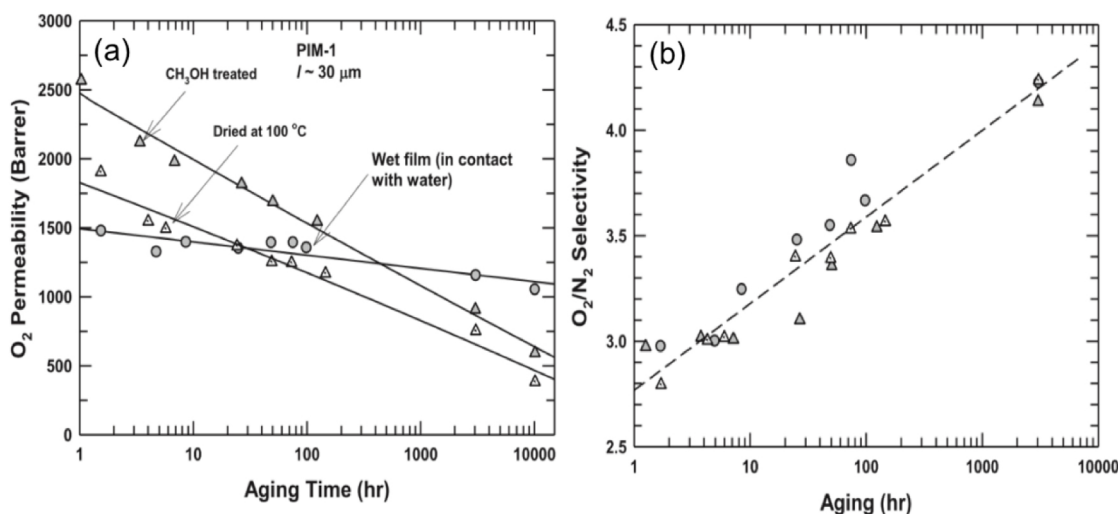

Figure 10. Time dependence of (a) O_2 permeability of and (b) O_2/N_2 selectivity of PIM-1 film [101].

Table 4. Gas permeation properties of PIMs MMMs. The maximum loading or loading yielding highest CO_2 permeability was selected if multiple loadings were reported. All data are adapted based on pure gas permeation unless specified. Loading are referring wt% unless specified (*vol%).

PIMs	Filler	Loading	Testing conditions	Permeability (P_i, Barrer)				Selectivity ($\alpha_{i/j}=P_i/P_j$)					Reference
				H_2	He	O_2	CO_2	$\alpha_{H2/N2}$	$\alpha_{He/N2}$	$\alpha_{O2/N2}$	$\alpha_{CO2/N2}$	$\alpha_{CO2/CH4}$	
PIM-1	Silica	23.5	23 °C, 3.4 bars	7190	2940	3730	13400	4.0	1.6	2.1	7.5	-	[75]
PIM-1	Silica	40	22 °C, 4 bars	5544	-	1734	8505	9.5	-	3.0	14.6	10.2	[77]
TOX-PIM-1	Silica	20	22 °C, 4 bars, crosslinked	2816	-	603	2615	28.0	-	6.0	26.0	32.5	[77]
PIM-1	Silicalite-1	35.5	25 °C, 1 bar	894	-	351	2530	10.8	-	4.2	30	13.8	[76]
PIM-1	Carbon nanotube	2	27 °C, 2 bars	-	-	605	7090	-	-	2.8	32.9	10.4	[78]
PIM-1	g-C_3N_4	1	30 °C, 2 bars, alcohol treated	5720	-	-	10528	-	-	-	13.8	8.3	[80]
PIM-1	Ion liquid	10	30 °C, 0.5 bar	-	-	101	812	-	-	3.7	30.1	18.9	[83]
PIM-1	ZIF-8	43*	20-22 °C, 1 bar, ethanol treated	14430	5990	5810	19350	8.2	3.4	3.3	11.0	7.3	[84]
PIM-1	ZIF-8	30	22 °C, 4 bars	5456	-	1452	6424	17.9	-	4.8	21.1	17.4	[77]
PIM-1	ZIF-8	20	22 °C, 4 bars, crosslinked	3465	-	800	3944	24.9	-	5.7	28.3	26.8	[77]
PIM-1	ZIF-8	10 cycles	25 °C, 1 bar	76	59	12	70	23.2	18.1	3.6	21.3	17.9	[91]
HMDA-PIM-1	HKUST-1	5 days	25 °C, 1 bar,	360	222	74.8	453	19.9	12.3	4.1	25.0	21.1	[91]
PIM-1	MIL-101	33*	NA	-	1200	1010	8440	-	6.8	4.0	36	-	[89]
PIM-1	ZIF-71	30	35 °C, 3.5 bars	-	-	1602	8377	-	-	3.5	18.3	11.2	[90]
PIM-1	CuBDC	10	25 °C, 1 bar, mixed gas	-	-	-	407 (GPU)	-	-	-	-	15.6	[92]
PIM-1	UiO-66	4.6	25 °C, 2 bars	3590	-	-	5340	14.4	-	-	21.4	17.2	[85]
PIM-1	Ti-UiO-66	13.3	25 °C, 2 bars	8380	-	-	14740	8.0	-	-	14.0	10.6	[85]
PIM-1	UiO-66	28.6	25 °C, 1 bar	6280	2380	2150	10900	8.8	4.0	3.0	15.2	3.2	[86]
PIM-1	UiO-66	30	35 °C, 1 bar	-	-	-	9420	-	-	-	15.6	12.3	[87]
PIM-1	UiO-66	20	25 °C, 4 bars	2730	-	1370	6981	5.1	-	2.6	13.0	9.3	[88]
PIM-1	COF	15	30 °C, 2 bars	-	-	-	7954	-	-	-	19.9	11.5	[93]

Table 5. Hollow fiber PIMs membranes gas separation performance based on pure gas permeation unless specified, compared to Matrimid®, Ultem, polysulfone and Propane Diol Monoester Cross-linkable (PDMC) polymer. Hollow fiber modules were not post-treated to reflect intrinsic gas separation properties. All data are based on pure gas permeation. l refers the skin layer thickness of hollow fiber membranes.

| Polymer	Polymer composition	Testing conditions	Permeance (P_i/l, GPU)		Selectivity ($\alpha_{i/j}=(P_i/l)/(P_j/l)$)			Reference
			O_2	CO_2	$\alpha_{O2/N2}$	$\alpha_{CO2/N2}$	$\alpha_{CO2/CH4}$	
PIM-1	PIM-1: Matrimid® (5:95)	Ambient temperature, 1 bar	39.5	172.9	5.4	23.8	22.4	[96]
PIM-1	PIM-1: Matrimid® (15:85)	Ambient temperature, 1 bar	33.5	413.2	1.6	5.1	6.1	[96]
Matrimid®	Neat polymer	Ambient temperature, 1 bar	16.9	86.3	6.5	33.2	34.5	[96]
PIM-1	PIM-1: Ultem (5:95)	Ambient temperature, 3 bars	8.2	33.9	7.2	30.3	35.2	[97]
PIM-1	PIM-1: Ultem (15:85)	Ambient temperature, 3 bars	13.0	49.0	5.8	21.9	28.9	[97]
Ultem	Neat polymer	Ambient temperature, 3 bars	5.2	24.1	7.4	33.9	36.8	[97]
PIM-1	Neat polymer	35 °C, 6.9 bars	60	360	4.6	27.7	22.5	[98]
Polysulfone	Neat polymer	25 °C, 5 bars	14.8	78.1	6.5	34.4	31.0	[122]
PDMC	Neat polymer	35 °C, 6.9 bars	63	-	4.6	-	-	[113]
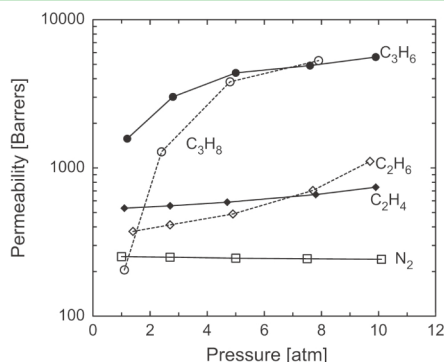
Figure 11. Penetrant permeability of PIM-1 as a function of pressure at 25 °C [105].

into PIMs polymer chains via chemical reaction to increase aging resistance[104]. These treatments aim to stiffen the polymer network and make the membrane more robust against aging, which, however, may increase the rigidity of PIMs - a potential issue for making mechanically flexible membranes. This fact notwithstanding, those techniques were found effective in deflecting aging curves of PIMs membranes and maintaining a high performance to an extended period of time.

3.2 Plasticization

Plasticization refers to a characteristic of polymeric membranes when gas fluxes increase with feeding pressures with a simultaneous loss of selectivity due to polymer swelling in the presence of highly sorbing components in the feed. As polymer chains are flexible, the sorbing component, also called plasticizer, dilates polymer chains, increasing the fractional free volume, shifting the polymer towards a rubberier regime, and causing a loss of separation efficacy. The species that cause plasticization include CO_2 [101] and certain hydrocarbons [105]. For instance, literatures studied effects of feeding pressures on hydrocarbon permeabilities of PIM-1 as **Figure 11** shows. The permeabilities of C_2H_4, C_2H_6, C_3H_6 and C_3H_8 rise with the feeding pressures, a strong indication of plasticization [105].

Multiple methods were postulated to hamper plasticization of PIMs membranes, such as cross-linking [61] and blending with POSS [103]. In particular, cross-linking is a straightforward approach to overcome plasticization accomplished by techniques introduced in Section 2.1.5 [106]. Despite the intrinsic rigidity of PIMs, plasticization is a practical issue that needs to be appropriately addressed for PIMs membranes, especially in the case of high pressure operation conditions.

3.3 Processability

PIM-1 is soluble in several organic solvents such as tetrahydrofuran (THF), chloroform and dichloromethane, which are therefore commonly used for flat-sheet membrane casting and hollow fiber membrane spinning. For example, PIM-1 was dissolved in THF and spun into hollow fiber membranes [98]. However, PIM-1 is insoluble in some polar solvents, such as N-methylpyrrolidone (NMP), dimethylacetamide (DMAc) and dimethylformamide (DMF) [107].

The insolubility of NMP or DMAc poses a challenge for processing PIMs into industrially relevant hollow fiber membranes since such solvents are often used for spinning hollow fibers [108]. However, researchers have identified approaches to modify PIMs to improve their solubility. Du et al reported

tetrazole and hydrolyzed PIM-1, which was soluble in NMP, making it possible to fabricate PIMs-based membranes from NMP solution [59, 107]. Mason et al explored thioamide modification of PIM-1 polymer, which was soluble in polar aprotic solvents such as DMAc, DMF and Dimethyl Sulfoxide [109]. This fact notwithstanding, gas fluxes of modified PIM-1 were found relatively lower than untreated PIM-1 [59, 107, 109]. Future work should address the permeability loss when increasing solubility in solvents by functionalizing PIMs.

3.4 Structure-property relationship

PIMs possess complicated microscale orientations, especially in the case of non-SBI-centered PIMs with bulky side groups, the pendent moieties can affect properties of PIMs appreciably. The irregular packing of polymer chains in ladder-like PIMs makes it difficult to predict the gas separation performance for a given structure. The large scattering permeability of PIM-1 shown in **Table 1** is an evidence of the challenge of obtaining identical gas separation properties of PIM-1 membrane from the same monomer. Potential reasons for the variability of permeation is that the permeability of PIMs is dependent of film thickness, post-treatment method (methanol or water soak), casting solution and of course, aging time [101].

It is important to note that PIMs, given that they are a kind of porous glassy polymer, have an inherent non-equilibrium behavior with a large amount of fractional free volume. As Section 3.1 discussed, the rapid aging caused by the non-equilibrium nature of PIMs suggests that the properties of PIMs are time-sensitive, which is another key parameter to consider when studying gas permeabilities of PIMs. Those aforementioned factors severely complicate the structure-property relationship in PIMs. It is, hence, difficult to unambiguously correlate the complicated relationship between the monomer structure, pore sizes, polymer fractional free volume and membrane gas separation properties [3].

Regardless of the challenge of correlating structure and property, several techniques were employed to explore PIMs microstructure evolution whilst examining gas separation properties. The pore size distributions and free volume in PIMs are often studied using Positron Annihilation Lifetime Spectroscopy (PALS), nitrogen adsorption, and molecular simulation [3, 99, 110, 111]. PALS is a non-destructive spectroscopy method to study the free volume of polymers. It is a useful technique to correlate the size of void volume of polymers with the lifetime of positronium. Pore size was also measured by using X-ray diffraction, including Small-angle X-ray scattering and Wide-angle X-ray scattering [112]. Future research in this field is essentially critical to understand PIMs in a molecular level and guide design of PIMs as a cutting-edge gas separation platform.

4 SUMMARY AND OUTLOOK

The discovery and development of PIMs opens the door into a burgeoning field with the potential to offer next-generation membranes with separation performance outcompeting conventional polymeric membranes. During the past two decades, PIMs have established themselves as an important class of microporous materials with hundreds of related papers and patent applications published. PIMs are widely recognized as

one of the most intrinsically permeable membrane materials, along with thermally rearranged polymers, and carbon molecular sieves. They have demonstrated superior high separation productivities with moderate selectivities crossing the Robeson upper bound remarkably.

Despite the intrinsically high separation productivity, there exist a number of technical barriers in PIMs membranes, such as physical aging, plasticization, processability, and more fundamental issues such as the lack of detailed structure-property relationships. Opportunities rely on properly overcoming those challenges. To date, studies on PIMs have been primarily focusing on dense film membranes. Only a handful papers or patents discussed the development of hollow fiber PIMs membranes. The fact that PIMs are not readily soluble in common solvents, like NMP and DMAc, may undermine the spinnability and manufacturability of PIMs into hollow fiber membranes, potentially hindering successful applicability of PIMs membranes in an industrial scale. Although PIMs have relatively lower selectivities compared to other glassy polymers, it remains promising to incorporate PIMs with molecularly sieving materials, such as selective polymers and inorganic fillers, to establish a percolative network to achieve both high flux and selectivity. It is foreseeable that PIMs will become a key player in membrane community when those issues can be successfully addressed.

Acknowledgements

Notes

The authors declare no competing financial interest.

References

[1] Canghai Ma; William J. Koros, High-performance ester-cross-linked hollow fiber membranes for natural gas separations. Journal of Membrane Science. 428, 251 (2013). doi:10.1016/j.memsci.2012.10.024

[2] P. Bernardo; E. Drioli; G. Golemme, Membrane Gas Separation: A Review/State of the Art. Industrial & Engineering Chemistry Research. 48(10), 4638 (2009). doi:10.1021/ie8019032

[3] Peter M. Budd; Neil B. McKeown, Highly permeable polymers for gas separation membranes. Polymer Chemistry. 1(1), (2010). doi:10.1039/b9py00319c

[4] Neil B. McKeown, Polymers of Intrinsic Microporosity. ISRN Materials Science. 2012, 1 (2012). doi:10.5402/2012/513986

[5] P. M. Budd; E. S. Elabas; B. S. Ghanem; S. Makhseed; N. B. McKeown; K. J. Msayib; C. E. Tattershall; D. Wang, Solution-processed, organophilic membrane derived from a polymer of intrinsic microporosity. Advanced Materials. 16(5), 456 (2004). doi:10.1002/adma.200306053

[6] L. M. Robeson, The upper bound revisited. Journal of Membrane Science. 320(1-2), 390 (2008). doi:10.1016/j.memsci.2008.04.030

[7] Y. Wang; N. B. McKeown; K. J. Msayib; G. A. Turnbull; I. D. W. Samuel, Laser Chemosensor with Rapid Responsivity and Inherent Memory Based on a Polymer of Intrinsic Microporosity. Sensors. 11(3), 2478 (2011). doi:10.3390/s110302478

[8] N. B. McKeown; P. M. Budd; K. J. Msayib; B. S. Ghanem; H. J. Kingston; C. E. Tattershall; S. Makhseed; K. J. Reynolds; D. Fritsch, Polymers of Intrinsic Microporosity (PIMs): Bridging the Void between Microporous and Polymeric Materials. Chemistry-a European Journal. 11(9), 2610 (2005). doi:10.1002/chem.200400860

[9] N. B. McKeown; B. S. Ghanem; K. J. Msayib; P. M. Budd; C. E. Tattershall; K. Mahmood; S. Tan; D. Book; H. W. Langmi; A. Walton, Towards polymer-based hydrogen storage materials: Engineering ultramicroporous cavities within polymers of intrinsic microporosity. Angewandte Chemie-International Edition. 45(11), 1804 (2006). doi:10.1002/anie.200504241

[10] K. J. Msayib; D. Book; P. M. Budd; N. Chaukura; K. D. M. Harris; M. Helliwell; S. Tedds; A. Walton; J. E. Warren; M. C. Xu; N. B. McKeown, Nitrogen and Hydrogen Adsorption by an Organic Microporous Crystal. Angewandte Chemie-International Edition. 48(18), 3273 (2009). doi:10.1002/anie.200900234

[11] Canghai Ma; William J. Koros, Ester-Cross-linkable Composite Hollow Fiber Membranes for CO_2 Removal from Natural Gas. Industrial & Engineering Chemistry Research. 52(31), 10495 (2013). doi:10.1021/ie303531r

[12] H. A. Mannan; H. Mukhtar; T. Murugesan; R. Nasir; D. F. Mohshim; A. Mushtaq, Recent Applications of Polymer Blends in Gas Separation Membranes. Chemical Engineering & Technology. 36(11), 1838 (2013). doi:10.1002/ceat.201300342

[13] L. M. Robeson, Polymer Blends in Membrane Transport Processes. Industrial & Engineering Chemistry Research. 49(23), 11859 (2010). doi:10.1021/ie100153q

[14] Lin Hao; Pei Li; Tai-Shung Chung, PIM-1 as an organic filler to enhance the gas separation performance of Ultem polyetherimide. Journal of Membrane Science. 453, 614 (2014). doi:10.1016/j.memsci.2013.11.045

[15] W. F. Yong; F. Y. Li; Y. C. Xiao; P. Li; K. P. Pramoda; Y. W. Tong; T. S. Chung, Molecular engineering of PIM-1/Matrimid blend membranes for gas separation. Journal of Membrane Science. 407, 47 (2012). doi:10.1016/j.memsci.2012.03.038

[16] W. F. Yong; Z. K. Lee; T. S. Chung; M. Weber; C. Staudt; C. Maletzko, Blends of a Polymer of Intrinsic Microporosity and Partially Sulfonated Polyphenylenesulfone for Gas Separation. Chemsuschem. 9(15), 1953 (2016). doi:10.1002/cssc.201600354

[17] Guangxi Dong; Hongyu Li; Vicki Chen, Challenges and opportunities for mixed-matrix membranes for gas separation. Journal of Materials Chemistry A. 1(15), (2013). doi:10.1039/c3ta00927k

[18] R. H. B. Bouma; A. Checchetti; G. Chidichimo; E. Drioli, Permeation through a heterogeneous membrane: The effect of the dispersed phase. Journal of Membrane Science. 128(2), 141 (1997). doi:10.1016/S0376-7388(96)00303-1

[19] N. C. Su; D. T. Sun; C. M. Beavers; D. K. Britt; W. L. Queen; J. J. Urban, Enhanced permeation arising from dual transport pathways in hybrid polymer-MOF membranes. Energy & Environmental Science. 9(3), 922 (2016). doi:10.1039/c5ee02660a

[20] P. M. Budd; N. B. McKeown, Recent developments in polymers of intrinsic microporosity. Abstracts of Papers of the American Chemical Society. 238, (2009).

[21] C. G. Bezzu; M. Carta; A. Tonkins; J. C. Jansen; P. Bernardo; F. Bazzarelli; N. B. McKeown, A spirobifluorene-based polymer of intrinsic microporosity with improved performance for gas separation. Adv Mater. 24(44), 5930 (2012). doi:10.1002/adma.201202393

[22] I. Rose; C. G. Bezzu; M. Carta; B. Comesana-Gandara; E. Lasseguette; M. C. Ferrari; P. Bernardo; G. Clarizia; A. Fuoco; J. C.

Jansen; K. E. Hart; T. P. Liyana-Arachchi; C. M. Colina; N. B. McKeown, Polymer ultrapermeability from the inefficient packing of 2D chains. Nature Materials. 16(9), 932 (2017). doi:10.1038/nmat4939

[23] P. Budd; K. Msayib; C. Tattershall; B. Ghanem; K. Reynolds; N. McKeown; D. Fritsch, Gas separation membranes from polymers of intrinsic microporosity. Journal of Membrane Science. 251(1-2), 263 (2005). doi:10.1016/j.memsci.2005.01.009

[24] M. Carta; R. Malpass-Evans; M. Croad; Y. Rogan; J. C. Jansen; P. Bernardo; F. Bazzarelli; N. B. McKeown, An efficient polymer molecular sieve for membrane gas separations. Science. 339(6117), 303 (2013). doi:10.1126/science.1228032

[25] Elena Tocci; Luana De Lorenzo; Paola Bernardo; Gabriele Clarizia; Fabio Bazzarelli; Neil B. McKeown; Mariolino Carta; Richard Malpass-Evans; Karel Friess; Kryštof Pilnáček; Marek Lanč; Yuri P. Yampolskii; Ludmila Strarannikova; Viktor Shantarovich; Michele Mauri; Johannes C. Jansen, Molecular Modeling and Gas Permeation Properties of a Polymer of Intrinsic Microporosity Composed of Ethanoanthracene and Tröger's Base Units. Macromolecules. 47(22), 7900 (2014). doi:10.1021/ma501469m

[26] Zheng Gong Wang; Xia Liu; Dong Wang; Jian Jin, Tröger's base-based copolymers with intrinsic microporosity for CO_2 separation and effect of Tröger's base on separation performance. Polymer Chemistry. 5(8), (2014). doi:10.1039/c3py01608k

[27] Mariolino Carta; Richard Malpass-Evans; Matthew Croad; Yulia Rogan; Michael Lee; Ian Rose; Neil B. McKeown, The synthesis of microporous polymers using Tröger's base formation. Polym. Chem. 5(18), 5267 (2014). doi:10.1039/c4py00609g

[28] Mariolino Carta; Matthew Croad; Johannes C. Jansen; Paola Bernardo; Gabriele Clarizia; Neil B. McKeown, Synthesis of cardo-polymers using Tröger's base formation. Polymer Chemistry. 5(18), (2014). doi:10.1039/c4py00607k

[29] Youchang Xiao; Liling Zhang; Li Xu; Tai-Shung Chung, Molecular design of Tröger's base-based polymers with intrinsic microporosity for gas separation. Journal of Membrane Science. 521, 65 (2017). doi:10.1016/j.memsci.2016.08.052

[30] M. Carta; M. Croad; R. Malpass-Evans; J. C. Jansen; P. Bernardo; G. Clarizia; K. Friess; M. Lanc; N. B. McKeown, Triptycene induced enhancement of membrane gas selectivity for microporous Troger's base polymers. Adv Mater. 26(21), 3526 (2014). doi:10.1002/adma.201305783

[31] O. Salinas; X. H. Ma; E. Litwiller; I. Pinnau, Ethylene/ethane permeation, diffusion and gas sorption properties of carbon molecular sieve membranes derived from the prototype ladder polymer of intrinsic microporosity (PIM-1). Journal of Membrane Science. 504, 133 (2016). doi:10.1016/j.memsci.2015.12.052

[32] Bader S. Ghanem; Neil B. McKeown; Peter M. Budd; Nasser M. Al-Harbi; Detlev Fritsch; Kathleen Heinrich; Ludmila Starannikova; Andrei Tokarev; Yuri Yampolskii, Synthesis, Characterization, and Gas Permeation Properties of a Novel Group of Polymers with Intrinsic Microporosity: PIM-Polyimides. Macromolecules. 42(20), 7881 (2009). doi:10.1021/ma901430q

[33] B. S. Ghanem; R. Swaidan; E. Litwiller; I. Pinnau, Ultra-microporous triptycene-based polyimide membranes for high-performance gas separation. Adv Mater. 26(22), 3688 (2014). doi:10.1002/adma.201306229

[34] Nasser Alaslai; Bader Ghanem; Fahd Alghunaimi; Ingo Pinnau, High-performance intrinsically microporous dihydroxyl-functionalized triptycene-based polyimide for natural gas separation. Polymer. 91, 128 (2016). doi:10.1016/j.polymer.2016.03.063

[35] Yulia Rogan; Richard Malpass-Evans; Mariolino Carta; Michael Lee; Johannes C. Jansen; Paola Bernardo; Gabriele Clarizia; Elena Tocci; Karel Friess; Marek Lanč; Neil B. McKeown, A highly

permeable polyimide with enhanced selectivity for membrane gas separations. J. Mater. Chem. A. 2(14), 4874 (2014). doi:10.1039/c4ta00564c

[36] Xiaohua Ma; Mahmoud A. Abdulhamid; Ingo Pinnau, Design and Synthesis of Polyimides Based on Carbocyclic Pseudo-Tröger's Base-Derived Dianhydrides for Membrane Gas Separation Applications. Macromolecules. 50(15), 5850 (2017). doi:10.1021/acs.macromol.7b01054

[37] Xiaohua Ma; Octavio Salinas; Eric Litwiller; Ingo Pinnau, Pristine and thermally-rearranged gas separation membranes from novel o-hydroxyl-functionalized spirobifluorene-based polyimides. Polym. Chem. 5(24), 6914 (2014). doi:10.1039/c4py01221f

[38] Shuangjiang Luo; Qiang Liu; Baohua Zhang; Jennifer R. Wiegand; Benny D. Freeman; Ruilan Guo, Pentiptycene-based polyimides with hierarchically controlled molecular cavity architecture for efficient membrane gas separation. Journal of Membrane Science. 480, 20 (2015). doi:10.1016/j.memsci.2015.01.043

[39] Xiaohua Ma; Raja Swaidan; Youssef Belmabkhout; Yihan Zhu; Eric Litwiller; Mustapha Jouiad; Ingo Pinnau; Yu Han, Synthesis and Gas Transport Properties of Hydroxyl-Functionalized Polyimides with Intrinsic Microporosity. Macromolecules. 45(9), 3841 (2012). doi:10.1021/ma300549m

[40] Zhenggong Wang; Dong Wang; Feng Zhang; Jian Jin, Tröger's Base-Based Microporous Polyimide Membranes for High-Performance Gas Separation. ACS Macro Letters. 3(7), 597 (2014). doi:10.1021/mz500184z

[41] N. Alaslai; X. Ma; B. Ghanem; Y. Wang; F. Alghunaimi; I. Pinnau, Synthesis and Characterization of a Novel Microporous Dihydroxyl-Functionalized Triptycene-Diamine-Based Polyimide for Natural Gas Membrane Separation. Macromol Rapid Commun. 38(18), (2017). doi:10.1002/marc.201700303

[42] Bader Ghanem; Nasser Alaslai; Xiaohe Miao; Ingo Pinnau, Novel 6FDA-based polyimides derived from sterically hindered Tröger's base diamines: Synthesis and gas permeation properties. Polymer. 96, 13 (2016). doi:10.1016/j.polymer.2016.04.068

[43] Michael Lee; C. Grazia Bezzu; Mariolino Carta; Paola Bernardo; Gabriele Clarizia; Johannes C. Jansen; Neil B. McKeown, Enhancing the Gas Permeability of Tröger's Base Derived Polyimides of Intrinsic Microporosity. Macromolecules. 49(11), 4147 (2016). doi:10.1021/acs.macromol.6b00351

[44] Shouliang Yi; Xiaohua Ma; Ingo Pinnau; William J. Koros, A high-performance hydroxyl-functionalized polymer of intrinsic microporosity for an environmentally attractive membrane-based approach to decontamination of sour natural gas. Journal of Materials Chemistry A. 3(45), 22794 (2015). doi:10.1039/c5ta05928c

[45] Yongbing Zhuang; Jong Geun Seong; Yu Seong Do; Hye Jin Jo; Zhaoliang Cui; Jongmyeong Lee; Young Moo Lee; Michael D. Guiver, Intrinsically Microporous Soluble Polyimides Incorporating Tröger's Base for Membrane Gas Separation. Macromolecules. 47(10), 3254 (2014). doi:10.1021/ma5007073

[46] Yongbing Zhuang; Jong Geun Seong; Yu Seong Do; Won Hee Lee; Moon Joo Lee; Michael D. Guiver; Young Moo Lee, High-strength, soluble polyimide membranes incorporating Tröger's Base for gas separation. Journal of Membrane Science. 504, 55 (2016). doi:10.1016/j.memsci.2015.12.057

[47] Y. Zhuang; J. G. Seong; Y. S. Do; W. H. Lee; M. J. Lee; Z. Cui; A. E. Lozano; M. D. Guiver; Y. M. Lee, Soluble, microporous, Troger's Base copolyimides with tunable membrane performance for gas separation. Chem Commun (Camb). 52(19), 3817 (2016). doi:10.1039/c5cc09783e

[48] Zhenggong Wang; Dong Wang; Jian Jin, Microporous Polyimides with Rationally Designed Chain Structure Achieving High Per-

formance for Gas Separation. Macromolecules. 47(21), 7477 (2014). doi:10.1021/ma5017506

[49] Shenghai Li; Hye Jin Jo; Sang Hoon Han; Chi Hoon Park; Seungju Kim; Peter M. Budd; Young Moo Lee, Mechanically robust thermally rearranged (TR) polymer membranes with spirobisindane for gas separation. Journal of Membrane Science. 434, 137 (2013). doi:10.1016/j.memsci.2013.01.011

[50] P. M. Budd; B. S. Ghanem; S. Makhseed; N. B. McKeown; K. J. Msayib; C. E. Tattershall, Polymers of intrinsic microporosity (PIMs): robust, solution-processable, organic nanoporous materials. Chem Commun (Camb). (2), 230 (2004). doi:10.1039/b311764b

[51] Ian Rose; Mariolino Carta; Richard Malpass-Evans; Maria-Chiara Ferrari; Paola Bernardo; Gabriele Clarizia; Johannes C. Jansen; Neil B. McKeown, Highly Permeable Benzotriptycene-Based Polymer of Intrinsic Microporosity. ACS Macro Letters. 4(9), 912 (2015). doi:10.1021/acsmacrolett.5b00439

[52] M. Carta; C. G. Bezzu; J. Vile; B. M. Kariuki; N. B. McKeown, Polymers of Intrinsic Microporosity derived from a carbocyclic analogue of Troger's base. Polymer. 126, 324 (2017). doi:10.1016/j.polymer.2017.03.037

[53] Xiaohua Ma; Ingo Pinnau, A novel intrinsically microporous ladder polymer and copolymers derived from 1,1′,2,2′-tetrahydroxy-tetraphenylethylene for membrane-based gas separation. Polymer Chemistry. 7(6), 1244 (2016). doi:10.1039/c5py01796c

[54] Mariolino Carta; Paola Bernardo; Gabriele Clarizia; Johannes C. Jansen; Neil B. McKeown, Gas Permeability of Hexaphenylbenzene Based Polymers of Intrinsic Microporosity. Macromolecules. 47(23), 8320 (2014). doi:10.1021/ma501925j

[55] Fu Yun Li; Youchang Xiao; Tai-Shung Chung; Sibudjing Kawi, High-Performance Thermally Self-Cross-Linked Polymer of Intrinsic Microporosity (PIM-1) Membranes for Energy Development. Macromolecules. 45(3), 1427 (2012). doi:10.1021/ma202667y

[56] Hongyong Zhao; Qian Xie; Xiaoli Ding; Jiangming Chen; Mingming Hua; Xiaoyao Tan; Yuzhong Zhang, High performance post-modified polymers of intrinsic microporosity (PIM-1) membranes based on multivalent metal ions for gas separation. Journal of Membrane Science. 514, 305 (2016). doi:10.1016/j.memsci.2016.05.013

[57] Q. Song; S. Cao; R. H. Pritchard; B. Ghalei; S. A. Al-Muhtaseb; E. M. Terentjev; A. K. Cheetham; E. Sivaniah, Controlled thermal oxidative crosslinking of polymers of intrinsic microporosity towards tunable molecular sieve membranes. Nat Commun. 5, 4813 (2014). doi:10.1038/ncomms5813

[58] Tom O. McDonald; Riaz Akhtar; Cher Hon Lau; Thanchanok Ratvijitvech; Ge Cheng; Rob Clowes; Dave J. Adams; Tom Hasell; Andrew I. Cooper, Using intermolecular interactions to crosslink PIM-1 and modify its gas sorption properties. Journal of Materials Chemistry A. 3(9), 4855 (2015). doi:10.1039/c4ta06070a

[59] Naiying Du; Mauro M. Dal-Cin; Gilles P. Robertson; Michael D. Guiver, Decarboxylation-Induced Cross-Linking of Polymers of Intrinsic Microporosity (PIMs) for Membrane Gas Separation. Macromolecules. 45(12), 5134 (2012). doi:10.1021/ma300751s

[60] N. Du; M. M. Cin; I. Pinnau; A. Nicalek; G. P. Robertson; M. D. Guiver, Azide-based cross-linking of polymers of intrinsic microporosity (PIMs) for condensable gas separation. Macromol Rapid Commun. 32(8), 631 (2011). doi:10.1002/marc.201000775

[61] Muntazim Munir Khan; Gisela Bengtson; Sergey Shishatskiy; Bahadir N. Gacal; Md Mushfequr Rahman; Silvio Neumann; Volkan Filiz; Volker Abetz, Cross-linking of Polymer of Intrinsic Microporosity (PIM-1) via nitrene reaction and its effect on gas transport property. European Polymer Journal. 49(12), 4157 (2013). doi:10.1016/j.eurpolymj.2013.09.022

[62] J. T. Liu; Y. C. Xiao; T. S. Chung, Flexible thermally treated 3D PIM-CD molecular sieve membranes exceeding the upper bound line for propylene/propane separation. Journal of Materials Chemistry A. 5(9), 4583 (2017). doi:10.1039/c6ta09751k

[63] Xiaohua Ma; Raja Swaidan; Baiyang Teng; Hua Tan; Octavio Salinas; Eric Litwiller; Yu Han; Ingo Pinnau, Carbon molecular sieve gas separation membranes based on an intrinsically microporous polyimide precursor. Carbon. 62, 88 (2013). doi:10.1016/j.carbon.2013.05.057

[64] Fu Yun Li; Youchang Xiao; Yee Kang Ong; Tai-Shung Chung, UV-Rearranged PIM-1 Polymeric Membranes for Advanced Hydrogen Purification and Production. Advanced Energy Materials. 2(12), 1456 (2012). doi:10.1002/aenm.201200296

[65] Q. Song; S. Cao; P. Zavala-Rivera; L. P. Lu; W. Li; Y. Ji; S. A. Al-Muhtaseb; A. K. Cheetham; E. Sivaniah, Photo-oxidative enhancement of polymeric molecular sieve membranes. Nat Commun. 4, 1918 (2013). doi:10.1038/ncomms2942

[66] Hosna Shamsipur; Bann A. Dawood; Peter M. Budd; Paola Bernardo; Gabriele Clarizia; Johannes C. Jansen, Thermally Rearrangeable PIM-Polyimides for Gas Separation Membranes. Macromolecules. 47(16), 5595 (2014). doi:10.1021/ma5011183

[67] Fu Yun Li; Tai-Shung Chung, Physical aging, high temperature and water vapor permeation studies of UV-rearranged PIM-1 membranes for advanced hydrogen purification and production. International Journal of Hydrogen Energy. 38(23), 9786 (2013). doi:10.1016/j.ijhydene.2013.05.056

[68] G. X. Dong; Y. M. Lee, Microporous polymeric membranes inspired by adsorbent for gas separation. Journal of Materials Chemistry A. 5(26), 13294 (2017). doi:10.1039/c7ta04015f

[69] T. Mitra; R. S. Bhavsar; D. J. Adams; P. M. Budd; A. I. Cooper, PIM-1 mixed matrix membranes for gas separations using cost-effective hypercrosslinked nanoparticle fillers. Chem Commun (Camb). 52(32), 5581 (2016). doi:10.1039/c6cc00261g

[70] Wai Fen Yong; Fu Yun Li; Tai Shung Chung; Yen Wah Tong, Molecular interaction, gas transport properties and plasticization behavior of cPIM-1/Torlon blend membranes. Journal of Membrane Science. 462, 119 (2014). doi:10.1016/j.memsci.2014.03.046

[71] Peyman Salehian; Wai Fen Yong; Tai-Shung Chung, Development of high performance carboxylated PIM-1/P84 blend membranes for pervaporation dehydration of isopropanol and CO_2/CH_4 separation. Journal of Membrane Science. 518, 110 (2016). doi:10.1016/j.memsci.2016.06.027

[72] X. M. Wu; Q. G. Zhang; P. J. Lin; Y. Qu; A. M. Zhu; Q. L. Liu, Towards enhanced CO_2 selectivity of the PIM-1 membrane by blending with polyethylene glycol. Journal of Membrane Science. 493, 147 (2015). doi:10.1016/j.memsci.2015.05.077

[73] L. X. Yang; Z. Z. Tian; X. Y. Zhang; X. Y. Wu; Y. Z. Wu; Y. N. Wang; D. D. Peng; S. F. Wang; H. Wu; Z. Y. Jiang, Enhanced CO_2 selectivities by incorporating CO_2-philic PEG-POSS into polymers of intrinsic microporosity membrane. Journal of Membrane Science. 543, 69 (2017). doi:10.1016/j.memsci.2017.08.050

[74] R. Castro-Munoz; V. Fila; C. T. Dung, Mixed Matrix Membranes Based on PIMs for Gas Permeation: Principles, Synthesis, and Current Status. Chemical Engineering Communications. 204(3), 295 (2017). doi:10.1080/00986445.2016.1273832

[75] Juhyeon Ahn; Wook-Jin Chung; Ingo Pinnau; Jingshe Song; Naiying Du; Gilles P. Robertson; Michael D. Guiver, Gas transport behavior of mixed-matrix membranes composed of silica nanoparticles in a polymer of intrinsic microporosity (PIM-1). Journal of Membrane Science. 346(2), 280 (2010). doi:10.1016/j.memsci.2009.09.047

[76] Christopher R. Mason; Maria Giovanna Buonomenna; Giovanni

Golemme; Peter M. Budd; Francesco Galiano; Alberto Figoli; Karel Friess; Vladimir Hynek, New organophilic mixed matrix membranes derived from a polymer of intrinsic microporosity and silicalite-1. Polymer. 54(9), 2222 (2013). doi:10.1016/j.polymer.2013.02.032

[77] Qilei Song; Shuai Cao; Robyn H. Pritchard; Hazim Qiblawey; Eugene M. Terentjev; Anthony K. Cheetham; Easan Sivaniah, Nano-filler-tuned microporous polymer molecular sieves for energy and environmental processes. Journal of Materials Chemistry A. 4(1), 270 (2016). doi:10.1039/c5ta09060a

[78] M. M. Khan; V. Filiz; G. Bengtson; S. Shishatskiy; M. Rahman; V. Abetz, Functionalized carbon nanotubes mixed matrix membranes of polymers of intrinsic microporosity for gas separation (vol 7, 504, 2012). Nanoscale Research Letters. 9, (2014). doi:10.1186/1556-276x-9-698

[79] K. Golzar; H. Modarress; S. Amjad-Iranagh, Effect of pristine and functionalized single- and multi-walled carbon nanotubes on CO_2 separation of mixed matrix membranes based on polymers of intrinsic microporosity (PIM-1): a molecular dynamics simulation study. J Mol Model. 23(9), 266 (2017). doi:10.1007/s00894-017-3436-3

[80] Zhizhang Tian; Shaofei Wang; Yutong Wang; Xiaorui Ma; Keteng Cao; Dongdong Peng; Xingyu Wu; Hong Wu; Zhongyi Jiang, Enhanced gas separation performance of mixed matrix membranes from graphitic carbon nitride nanosheets and polymers of intrinsic microporosity. Journal of Membrane Science. 514, 15 (2016). doi:10.1016/j.memsci.2016.04.019

[81] A. Gonciaruk; K. Althumayri; W. J. Harrison; P. M. Budd; F. R. Siperstein, PIM-1/graphene composite: A combined experimental and molecular simulation study. Microporous and Mesoporous Materials. 209, 126 (2015). doi:10.1016/j.micromeso.2014.07.007

[82] Kuo-Sung Liao; Juin-Yih Lai; Tai-Shung Chung, Metal ion modified PIM-1 and its application for propylene/propane separation. Journal of Membrane Science. 515, 36 (2016). doi:10.1016/j.memsci.2016.05.032

[83] Karabi Halder; Muntazim Munir Khan; Judith Grünauer; Sergey Shishatskiy; Clarissa Abetz; Volkan Filiz; Volker Abetz, Blend membranes of ionic liquid and polymers of intrinsic microporosity with improved gas separation characteristics. Journal of Membrane Science. 539, 368 (2017). doi:10.1016/j.memsci.2017.06.022

[84] Alexandra F. Bushell; Martin P. Attfield; Christopher R. Mason; Peter M. Budd; Yuri Yampolskii; Ludmila Starannikova; Alexander Rebrov; Fabio Bazzarelli; Paola Bernardo; Johannes Carolus Jansen; Marek Lanč; Karel Friess; Victor Shantarovich; Vadim Gustov; Vera Isaeva, Gas permeation parameters of mixed matrix membranes based on the polymer of intrinsic microporosity PIM-1 and the zeolitic imidazolate framework ZIF-8. Journal of Membrane Science. 427, 48 (2013). doi:10.1016/j.memsci.2012.09.035

[85] S. J. Smith; B. P. Ladewig; A. J. Hill; C. H. Lau; M. R. Hill, Post-synthetic Ti exchanged UiO-66 metal-organic frameworks that deliver exceptional gas permeability in mixed matrix membranes. Sci Rep. 5, 7823 (2015). doi:10.1038/srep07823

[86] Muhanned R. Khdhayyer; Elisa Esposito; Alessio Fuoco; Marcello Monteleone; Lidietta Giorno; Johannes C. Jansen; Martin P. Attfield; Peter M. Budd, Mixed matrix membranes based on UiO-66 MOFs in the polymer of intrinsic microporosity PIM-1. Separation and Purification Technology. 173, 304 (2017). doi:10.1016/j.seppur.2016.09.036

[87] Youzhi Cao; Qin Gao; Qiao Li; Xinbo Jing; Shufen Wang; Wei Wang, Synthesis of 3D porous $MoS_2/g-C_3N_4$ heterojunction as a high efficiency photocatalyst for boosting H_2 evolution activity. Rsc Advances. 7(65), 40727 (2017). doi:10.1039/c7ra06774g

[88] Behnam Ghalei; Kento Sakurai; Yosuke Kinoshita; Kazuki Wakimoto; Ali Pournaghshband Isfahani; Qilei Song; Kazuki Doitomi; Shuhei Furukawa; Hajime Hirao; Hiromu Kusuda; Susumu Kitagawa; Easan Sivaniah, Enhanced selectivity in mixed matrix membranes for CO_2 capture through efficient dispersion of amine-functionalized MOF nanoparticles. Nature Energy. 2(7), (2017). doi:10.1038/nenergy.2017.86

[89] A. Y. Alentiev; G. N. Bondarenko; Y. V. Kostina; V. P. Shantarovich; S. N. Klyamkin; V. P. Fedin; K. A. Kovalenko; Y. P. Yampolskii, PIM-1/MIL-101 Hybrid Composite Membrane Material: Transport Properties and Free Volume. Petroleum Chemistry. 54(7), 477 (2014). doi:10.1134/S0965544114070020

[90] Lin Hao; Kuo-Sung Liao; Tai-Shung Chung, Photo-oxidative PIM-1 based mixed matrix membranes with superior gas separation performance. Journal of Materials Chemistry A. 3(33), 17273 (2015). doi:10.1039/c5ta03776j

[91] A. Fuoco; M. R. Khdhayyer; M. P. Attfield; E. Esposito; J. C. Jansen; P. M. Budd, Synthesis and Transport Properties of Novel MOF/PIM-1/MOF Sandwich Membranes for Gas Separation. Membranes (Basel). 7(1), (2017). doi:10.3390/membranes7010007

[92] Y. D. Cheng; X. R. Wang; C. K. Jia; Y. X. Wang; L. Z. Zhai; Q. Wang; D. Zhao, Ultrathin mixed matrix membranes containing two-dimensional metal-organic framework nanosheets for efficient CO2/CH4 separation. Journal of Membrane Science. 539, 213 (2017). doi:10.1016/j.memsci.2017.06.011

[93] Xingyu Wu; Zhizhang Tian; Shaofei Wang; Dongdong Peng; Leixin Yang; Yingzhen Wu; Qingping Xin; Hong Wu; Zhongyi Jiang, Mixed matrix membranes comprising polymers of intrinsic microporosity and covalent organic framework for gas separation. Journal of Membrane Science. 528, 273 (2017). doi:10.1016/j.memsci.2017.01.042

[94] J. S. Mchattie; W. J. Koros; D. R. Paul, Gas-Transport Properties of Polysulfones: 1. Role of Symmetry of Methyl-Group Placement on Bisphenol Rings. Polymer. 32(5), 840 (1991). doi:10.1016/0032-3861(91)90508-G

[95] De Q. Vu; William J. Koros; Stephen J. Miller, Effect of condensable impurity in CO_2/CH_4 gas feeds on performance of mixed matrix membranes using carbon molecular sieves. Journal of Membrane Science. 221(1-2), 233 (2003). doi:10.1016/s0376-7388(03)00245-x

[96] W. F. Yong; F. Y. Li; Y. C. Xiao; T. S. Chung; Y. W. Tong, High performance PIM-1/Matrimid hollow fiber membranes for CO_2/CH_4, O_2/N_2 and CO_2/N_2 separation. Journal of Membrane Science. 443, 156 (2013). doi:10.1016/j.memsci.2013.04.037

[97] Lin Hao; Jian Zuo; Tai-Shung Chung, Formation of defect-free polyetherimide/PIM-1 hollow fiber membranes for gas separation. AIChE Journal. 60(11), 3848 (2014). doi:10.1002/aic.14565

[98] Melinda L. Jue; Victor Breedveld; Ryan P. Lively, Defect-free PIM-1 hollow fiber membranes. Journal of Membrane Science. 530, 33 (2017). doi:10.1016/j.memsci.2017.02.012

[99] P. Budd; N. McKeown; B. Ghanem; K. Msayib; D. Fritsch; L. Starannikova; N. Belov; O. Sanfirova; Y. Yampolskii; V. Shantarovich, Gas permeation parameters and other physicochemical properties of a polymer of intrinsic microporosity: Polybenzodioxane PIM-1. Journal of Membrane Science. 325(2), 851 (2008). doi:10.1016/j.memsci.2008.09.010

[100] P. Bernardo; F. Bazzarelli; F. Tasselli; G. Clarizia; C. R. Mason; L. Maynard-Atem; P. M. Budd; M. Lanč; K. Pilnáček; O. Vopička; K. Friess; D. Fritsch; Yu P. Yampolskii; V. Shantarovich; J. C. Jansen, Effect of physical aging on the gas transport and sorption in PIM-1 membranes. Polymer. 113, 283 (2017). doi:10.1016/j.polymer.2016.10.040

[101] Rajkiran R. Tiwari; Jianyong Jin; B. D. Freeman; D. R. Paul,

Physical aging, CO_2 sorption and plasticization in thin films of polymer with intrinsic microporosity (PIM-1). Journal of Membrane Science. 537, 362 (2017). doi:10.1016/j.memsci.2017.04.069

[102] C. H. Lau; K. Konstas; A. W. Thornton; A. C. Liu; S. Mudie; D. F. Kennedy; S. C. Howard; A. J. Hill; M. R. Hill, Gas-separation membranes loaded with porous aromatic frameworks that improve with age. Angew Chem Int Ed Engl. 54(9), 2669 (2015). doi:10.1002/anie.201410684

[103] Wai Fen Yong; Kar Hui Andrel Kwek; Kuo-Sung Liao; Tai-Shung Chung, Suppression of aging and plasticization in highly permeable polymers. Polymer. 77, 377 (2015). doi:10.1016/j.polymer.2015.09.075

[104] Jiangtao Liu; Youchang Xiao; Kuo-Sung Liao; Tai-Shung Chung, Highly permeable and aging resistant 3D architecture from polymers of intrinsic microporosity incorporated with beta-cyclodextrin. Journal of Membrane Science. 523, 92 (2017). doi:10.1016/j.memsci.2016.10.001

[105] Pei Li; T. S. Chung; D. R. Paul, Gas sorption and permeation in PIM-1. Journal of Membrane Science. 432, 50 (2013). doi:10.1016/j.memsci.2013.01.009

[106] Canghai Ma; William J. Koros, Effects of hydrocarbon and water impurities on CO_2/CH_4 separation performance of ester-crosslinked hollow fiber membranes. Journal of Membrane Science. 451, 1 (2014). doi:10.1016/j.memsci.2013.09.035

[107] Naiying Du; Michael D. Guiver; Gilles P. Robertson; Jingshe Song, Carboxylated polymers of intrinsic microporosity (PIMs) with tunable gas transport properties. US Patent. US8809488 B2 (2014)

[108] L. F. Kong; K. Li, Preparation of PVDF hollow-fiber membranes via immersion precipitation. Journal of Applied Polymer Science. 81(7), 1643 (2001). doi:10.1002/app.1595

[109] Christopher R. Mason; Louise Maynard-Atem; Nasser M. Al-Harbi; Peter M. Budd; Paola Bernardo; Fabio Bazzarelli; Gabriele Clarizia; Johannes C. Jansen, Polymer of Intrinsic Microporosity Incorporating Thioamide Functionality: Preparation and Gas Transport Properties. Macromolecules. 44(16), 6471 (2011). doi:10.1021/ma200918h

[110] Peter M. Budd; Neil B. McKeown; Detlev Fritsch, Free volume and intrinsic microporosity in polymers. Journal of Materials Chemistry. 15(20), 1977 (2005). doi:10.1039/b417402j

[111] Matthias Heuchel; Detlev Fritsch; Peter M. Budd; Neil B. McKeown; Dieter Hofmann, Atomistic packing model and free volume distribution of a polymer with intrinsic microporosity (PIM-1). Journal of Membrane Science. 318(1-2), 84 (2008). doi:10.1016/j.memsci.2008.02.038

[112] A. G. McDermott; P. M. Budd; N. B. McKeown; C. M. Colina; J. Runt, Physical aging of polymers of intrinsic microporosity: a SAXS/WAXS study. Journal of Materials Chemistry A. 2(30), 11742 (2014). doi:10.1039/c4ta02165g

[113] Canghai Ma; Chen Zhang; Ying Labreche; Shilu Fu; Lu Liu; William J. Koros, Thin-skinned intrinsically defect-free asymmetric mono-esterified hollow fiber precursors for crosslinkable polyimide gas separation membranes. Journal of Membrane Science. 493, 252 (2015). doi:10.1016/j.memsci.2015.06.018

[114] C. L. Staiger; S. J. Pas; A. J. Hill; C. J. Cornelius, Gas separation, free volume distribution, and physical aging of a highly microporous spirobisindane polymer. Chemistry of Materials. 20(8), 2606 (2008). doi:10.1021/cm071722t

[115] N. Y. Du; G. P. Robertson; J. S. Song; I. Pinnau; S. Thomas; M. D. Guiver, Polymers of Intrinsic Microporosity Containing Trifluoromethyl and Phenylsulfone Groups as Materials for Membrane Gas Separation. Macromolecules. 41(24), 9656 (2008). doi:10.1021/ma801858d

[116] Naiying Du; Gilles P. Robertson; Ingo Pinnau; Michael D. Guiver, Polymers of Intrinsic Microporosity with Dinaphthyl and Thianthrene Segments. Macromolecules. 43(20), 8580 (2010). doi:10.1021/ma101930x

[117] C. G. Bezzu; M. Carta; A. Tonkins; J. C. Jansen; P. Bernardo; F. Bazzarelli; N. B. McKeown, A Spirobifluorene-Based Polymer of Intrinsic Microporosity with Improved Performance for Gas Separation. Advanced Materials. 24(44), 5930 (2012). doi:10.1002/adma.201202393

[118] B. S. Ghanem; N. B. McKeown; P. M. Budd; J. D. Selbie; D. Fritsch, High-performance membranes from polyimides with intrinsic microporosity. Adv Mater. 20(14), 2766 (2008). doi:10.1002/adma.200702400

[119] Yulia Rogan; Ludmila Starannikova; Victoria Ryzhikh; Yuri Yampolskii; Paola Bernardo; Fabio Bazzarelli; Johannes Carolus Jansen; Neil B. McKeown, Synthesis and gas permeation properties of novel spirobisindane-based polyimides of intrinsic microporosity. Polymer Chemistry. 4(13), (2013). doi:10.1039/c3py00451a

[120] R. Short; M. Carta; C. G. Bezzu; D. Fritsch; B. M. Kariuki; N. B. McKeown, Hexaphenylbenzene-based polymers of intrinsic microporosity. Chem Commun (Camb). 47(24), 6822 (2011). doi:10.1039/c1cc11717c

[121] Wai Fen Yong; Tai-Shung Chung, Miscible blends of carboxylated polymers of intrinsic microporosity (cPIM-1) and Matrimid. Polymer. 59, 290 (2015). doi:10.1016/j.polymer.2015.01.013

[122] M. F. A. Wahab; A. F. Ismail; S. J. Shilton, Studies on gas permeation performance of asymmetric polysulfone hollow fiber mixed matrix membranes using nanosized fumed silica as fillers. Separation and Purification Technology. 86, 41 (2012). doi:10.1016/j.seppur.2011.10.018